"SAINT PETERSBURG STATE UNIVERSITY"

**Tiuterev Mikhail Ivanovich**

**Final qualifying work (English translated version. Correction is still in progress)**

# Analysis of numerical models describing the aging of lithium-ion batteries due to the formation of an interphase layer of solid electrolyte

Level of education: bachelor's degree
Direction: 03.03.01 “Applied Math and Physics”
Main educational program "Engineering-oriented physics"

Scientific adviser:
Ph.D., assistant, Vasilkov Sergey Andreevich
Reviewer:
Trainee-analyst, Tinkoff Bank JSC, Anastasia Vitalievna Slesarenko

Saint Petersburg, 2023

# Table of contents

# 1. Introduction

Currently, the issue of not only production, but also the correct supply and storage of energy is very acute. Each mobile device basically contains a battery that can withstand a certain number of recharges. Lithium-ion batteries in particular have high energy density, but they are more expensive than other types, are sensitive to overcharging, and can ignite or explode if damaged or overheated. If you make a good model of a battery, you can predict its behavior under different conditions and optimize its performance.

This work will consider a method for creating a battery model without additional degradation associated solely with the movement of lithium ions, and will simulate the processes of formation of an interfacial layer of solid electrolyte using COMSOL software packages.

The battery is represented as an electrical cell consisting of several basic elements: negative and positive electrodes, electrolyte and separator. Electrodes are metal, metal oxide or carbon on which oxidation processes take place or restoration when electric current flows. An electrolyte is an electro-neutral liquid filled with ions that provides connection between the electrodes. A separator is a layer that protects the electrodes from contact and short circuit.

The main mechanism of battery degradation is the interfacial layer at the interface of the electrode and electrolyte (Solid Electrolyte Interface, SEI or film) that appears on the surface of one of the electrodes. The formation of this film is associated with the reaction of the solvent entering the phase interface. Thickening the film leads to several effects: a decrease in the amount of active substance and an increase in battery resistance. Thickening of the film leads to an additional voltage drop, and as a result, to the release of heat, which in the future can lead to thermal runaway (uncontrolled heat release).

The main goal of the work is to create a numerical model of a lithium-ion battery capable of describing the rate of decline the quality of its characteristics. To achieve the goal, the following tasks were implemented:

- Search for characteristic parameter values in the literature
- Creation of a simple isothermal battery model based on porous electrode theory
- Implementation of different battery charging methods
- Description of the main degradation mechanism caused by the appearance of a film at the electrode boundary and its implementation
- Analysis of the obtained experimental data and search for dependencies affecting capacity loss

The practical significance of this work is the proposal of an approach to constructing a model of a lithium-ion battery, which takes into account the electrochemical processes inside the battery and the deterioration of its characteristics due to the growth of the interphase layer. The model helps to understand the reasons for the loss of capacity due to the formation of a film at the electrode boundary, and also to select the appropriate operating mode of the battery. In the future, when this model is integrated as a module into the calculation of the thermal problem, it will be possible to predict overheating of the battery due to additional heating on the formed film.

# 2. Literature review

## 2.1. Porous Electrode Theory Analysis

The electrodes in batteries do not have a continuous, but a heterogeneous structure due to the fact that they are made from many small particles. This is done to increase the surface area of the electrodes to facilitate the movement of lithium and reduce the overall resistance of the cell, thereby increasing the ability to deliver energy. For example, Figure 1 shows a scanning electron microscope image of an electrode made of graphite particles.

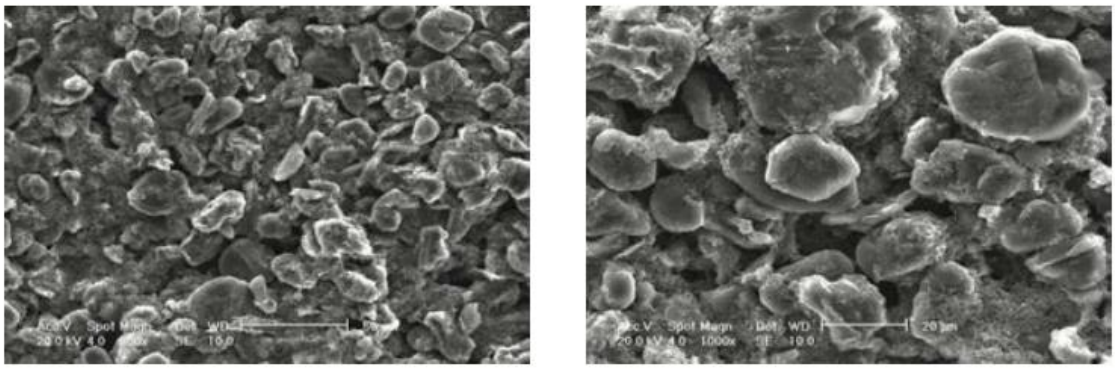

***Figure 1. Porous electrode geometry. Scanning electron microscope image [8]***

To solve the problem of modeling the cyclic operation of a battery, Newman [1,2] proposed a simplification to the theory of a porous electrode. According to this theory, the equations of motion ions in liquid and solid media will be similar to the corresponding classical equations, with some changes in the coefficients.

Let us consider the porous electrode model itself. A porous electrode is an element that includes both an electrode and an electrolyte material. It is defined as the union of these two states. The abstraction is shown in Figure 2. At each point of the electrolyte there is a boundary of a spherical electrode particle (of radius R with a radial distribution of lithium ions). When a lithium ion moves through the electrolyte, it can go into a solid electrode, or further move through the electrolyte. To describe the motion of lithium inside solid particles, a pseudo-space is introduced in which the motion of lithium is possible only along particle radius.

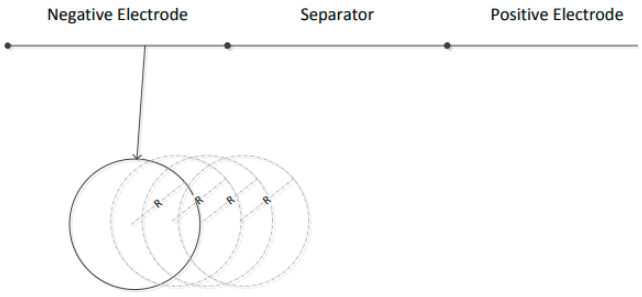


***Figure 2. Schematic representation of the basic geometry and pseudo-space [18]. Each point of the basic geometry (upper part of the figure) corresponds to a sphere with a spherically symmetric distribution of lithium ions. When a voltage is applied, the ion can exit the ball into the underlying geometry, and vice versa.***

The electrochemical cell considered in the model is presented in Figure 3a and consists of 3 parts (positive electrode, negative electrode, separator).

The pseudo-space model is presented in Figure 3b in the form of two rectangles (A = length of the electrode, B = radius of the solid particle), each corresponding to its own electrode.

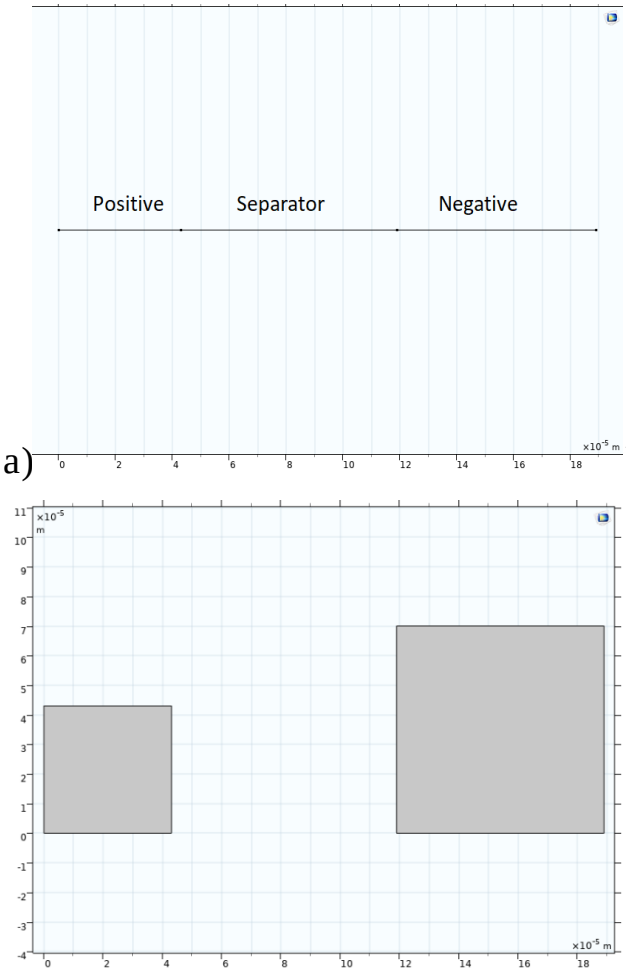


***Figure 3. Geometry of a computer cell model. a) Basic geometry, b) Pseudo-space.***

Lithium cobaltate LiCoO2 was adopted as the positive electrode. When a battery is charged, lithium ions leave the positive electrode and enter the negative electrode, which is made of carbon C6. A film consisting of electrolyte (ethylene decarbonate, EDC) is formed at the interface of the negative electrode and electrolyte [3], lithium ions and electrons from the solid electrode. Li2EDC connection forms a layer with lower (4-6 orders of magnitude) electrical conductivity (and, accordingly, higher resistivity by the same number of orders of magnitude), which leads to an additional voltage drop and causes heating of the battery as a whole. Also, this reaction irreversibly consumes active lithium [4], which can participate in charging/discharging processes.

At the electrode/electrolyte interface in the equilibrium position, a potential drop appears, called the open circuit voltage. This voltage can also be defined as the potential between the electrode and the electrolyte when no current is flowing, or the potential difference that must be applied to the system in order to compensate for the flow of lithium out and into the electrode. The data for the values were selected in the article [5].

$$(\varphi_s - \varphi_e)(t = 0) = U_{ocp}\left(\frac{c_s\,(0)}{c_{s\,max}}\right)$$

Where are the potentials in the solid and liquid phases, respectively, and is the open circuit potential. The dependence of these potentials on the concentration of lithium ions in the electrodes is presented in Figure 4.$\varphi_s$ ,$\varphi_e U_{ocp}$

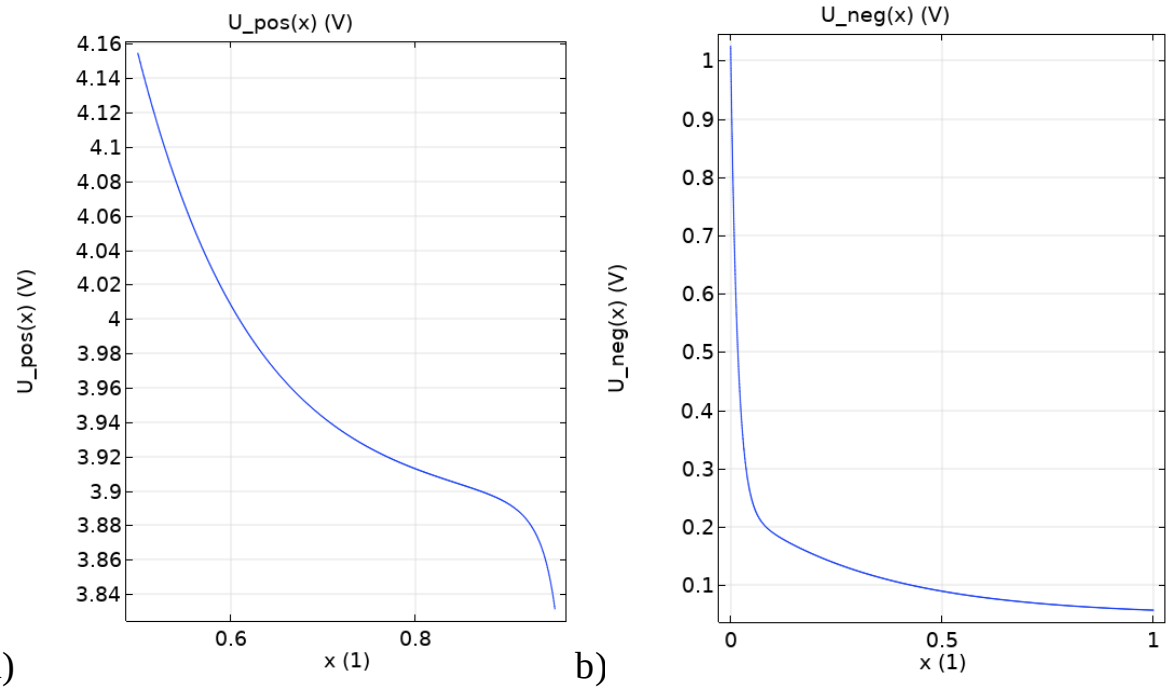


A) b)

***Figure 4. Graphs of open circuit potentials a) for positive b) for negative electrode***

For cobaltate, not the entire range of lithium concentrations is available, but only the second half $0.5 < \frac{c_s\,(t)}{c_{s\,max}} < 1$. This is due to the fact that half of the lithium ions stored in cobaltate are necessary to maintain the stability of its molecular structure. If you remove too much lithium from it, the structure will collapse, and

these irreversible changes will lead to the inability of lithium to penetrate the electrode.

## 2.2. Analysis of different film growth models

Film (SEI) is a key factor limiting battery life and capacity [6]. Despite a large number of studies on SEI, this layer is still not fully understood. This is due to the complex structure of the film, its highly heterogeneous structure, schematically presented in Figure 5.

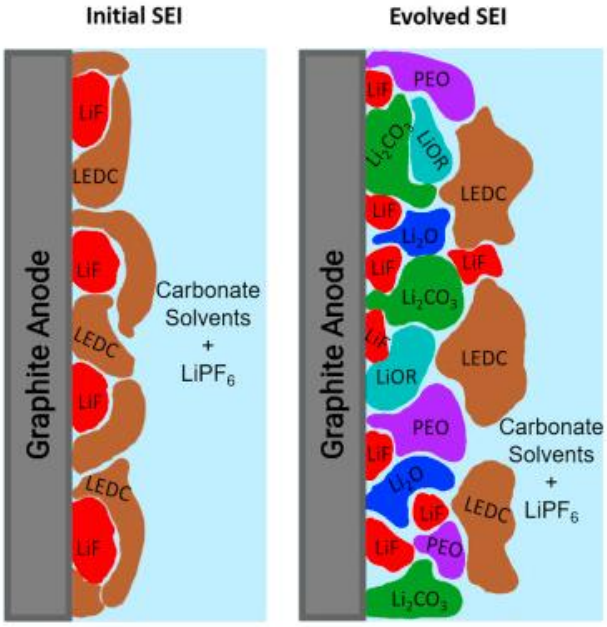


*Figure 5. Schematic representation of the SEI structure [7]*

Research agrees that the film formation process occurs at the electrode-electrolyte interface under the existing SEI layer [8,9].

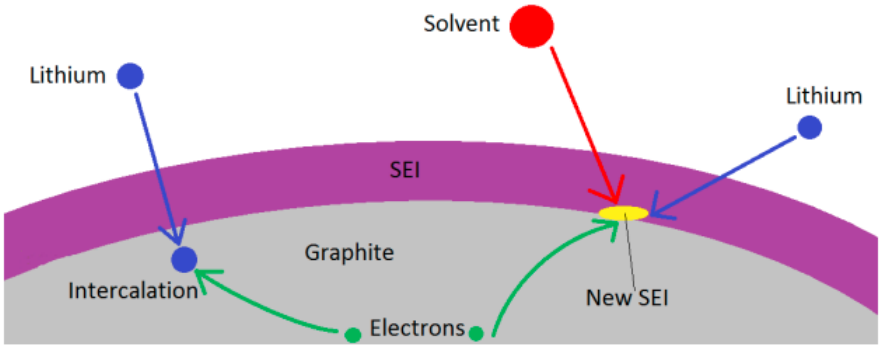


*Figure 6. Schematic representation of the film formation reaction [9]*

Most commonly the mechanism that determines the growth rate of the SEI layer is the diffusion of the solvent through the film layer [9]. Figure 6 shows a schematic

flow of processes in the film region. It should also be noted that there is an alternative approach associated with the tunneling of electrons necessary for the formation of a new layer [10,11]. According to this approach, electrons are able to penetrate the SEI layer on the negative electrode of the battery due to the quantum mechanical effect of tunneling. In this way, electrons can overcome a potential barrier that would normally prevent them from moving from the electrode to the electrolyte. In this formulation of the problem, electron tunneling promotes the growth of the SEI layer due to the reaction of electrons with the electrolyte components and the formation of various compounds on the anode surface and is an effect that determines the reaction rate.

In the current study, it was decided to use the first mechanism due to the more developed experimental base for modeling these processes. A detailed comparison of these two modeling mechanisms is presented in the article [11]. The main results of previous studies were that the drop in capacity on average across a battery can be described by a simplified model, replacing the pseudo-space with one averaged particle, however, at high current and large electrode sizes, it is necessary to take into account the spatial distribution and use the theory of a porous electrode [9]. It was also found that the SEI layer grows rapidly to a stable state during the first few charge/discharge cycles, and the growth rate varies with the phase of the cycle. The slowdown in layer growth is presumably associated with restrictions on the diffusion of the electrolyte through the already formed layer [14]. For the charge-discharge cycle, the characteristic dependence of film growth on the cycle was determined in [14] (Figure 7). In the future, when analyzing the data, we will evaluate whether the nature of the dependence is similar.

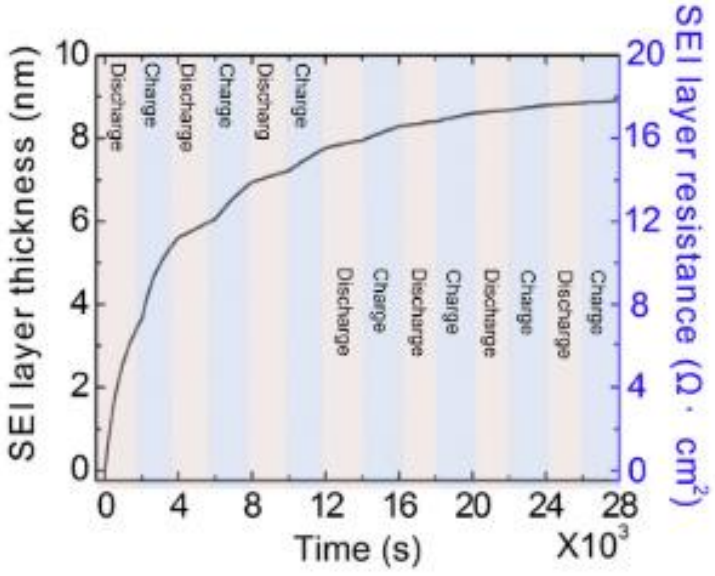


***Figure 7. Characteristic dynamic dependence of film growth during a charge-discharge cycle [14]***

In [15], a model of aging of a graphite electrode was considered based on a combination of two components: flow through the cracked part and diffusion through the uncracked part of the SEI layer. This amendment had an impact on the results obtained, but no comparison was made with the results of other articles.

## 2.3. Analysis of film growth in conjunction with temperature

This work investigates the effect of SEI film growth side reaction on the performance of Li-ion batteries under different charging methods. SEI film growth is one of the main factors affecting battery aging as it increases the ohmic resistance of the battery and reduces the amount of active lithium in it. To analyze SEI film growth, an electrochemical battery model was developed that takes into account this film formation mechanism. The model allows us to evaluate the distribution of SEI film thickness on the electrode surface and its effect on battery performance.

In addition to SEI film growth, battery capacity is also affected by temperature, which determines the rate of chemical reactions and material properties. Previously, several thermo-electrochemical models have been developed to study the temperature distribution and its effect on cell performance, but the SEI layer in them was either ignored or simplified to a constant resistance [12,13]. Subsequently, by adding temperature changes to the model and taking into account the dependence of

material properties on temperature, it becomes possible to consider the combined effect of temperature and film growth on battery performance. However, this is beyond the scope of this study.

## 2.4. Analysis of kinetic equations for film growth

To define the equation for the growth of SEI, the Butler-Volmer kinetic equation is usually used. It shows how the rate of reaction at an electrode depends on the applied voltage and on the characteristics on the surface of the electrode.

$$j = \frac{i_0}{F}\left(\exp\left(-\frac{\alpha F}{RT}\eta_1\right) - \exp\left(\frac{\alpha F}{RT}\eta_2\right)\right) \quad (1a)$$

where $i_0 = F \cdot k_{sei\ norm}\left(\frac{c_{elec}(x,t)}{c_0} \cdot \frac{c_e(x,t)}{c_{e0}}\right)^{\alpha}$ initial value of current density, $k_{\text{sei }norm}$ – reaction coefficient, $\alpha$ – transfer coefficient, $\eta_1, \eta_2$ – overvoltage.

Depending on the presence of a reverse reaction, this equation takes a symmetrical [9] or asymmetrical form [14,15,16] in the case of irreversible reactions. The assumption that the reaction is irreversible is confirmed by experimental research [17], so we will limit ourselves to modeling an irreversible reaction.

$$j_{sei} = \frac{i_0}{F} \cdot \exp\left(-\frac{\alpha F}{RT}\eta_{sei}\right) \quad (1b)$$

Another important result of the study [17] is the growth of the film at any value of overvoltage, and the growth rate drops when the electrolyte reduction potential is reached $U_{elec} = 0.8\,V$ [6].

The expression for determining overvoltage is defined differently in different documentary sources. It is associated with a drop in potential at the interface of the electrode and electrolyte. In most cases, this voltage is defined as $\eta_{sei} = \varphi_s - \varphi_e - U_{sei} - dphi$ where $dphi$ is the voltage drop across the film. $U_{sei}$ takes values 0 [14], 0.4 [16], 0.8 [9], $\varphi_s$ [15]. However, the data determined by a constant value may not contradict each other, because additional terms in exponential (1b) can go into the reaction constant $i_0$ during an irreversible process.

## 2.5. Determining coefficients for equations

Different types of the Butler-Volmer equation leads to different values of reaction coefficients presented in the literature. Data on the reaction coefficient may differ by several orders of magnitude due to the fact that, in my opinion, it was set implicitly by the authors of the articles. For example, in [14] it is not normalized to the maximum concentration, but in [16] it is specified not $k_{sei\ norm}$ , but $i_0$. And the reaction coefficient itself has already been recalculated based on the existing value. It was decided to choose the value $k_{sei\ norm} = 2 \cdot 10^{-14} \frac{mol}{m^2 \cdot s}$ [16] for the model.

Basically, the diffusion coefficients of electrolyte through SEI were taken at the value $D_{sei} = 10^{-13} \frac{m^2}{s}$ [14]. However, this value of the diffusion coefficient is approximately the same order as the diffusion of lithium in solid particles $D_+ = 3 \cdot 10^{-14} \frac{m^2}{s}, D_- = 10^{-13} \frac{m^2}{s}$, and the passage of the electrolyte through the film layer is not decisive during the formation of a new film. Data on the diffusion coefficient of the electrolyte through the film layer, as well as its dependence on temperature, were obtained based on extrapolation of the graph (Figure 8) of the dependence of this coefficient on temperature in the article [17].

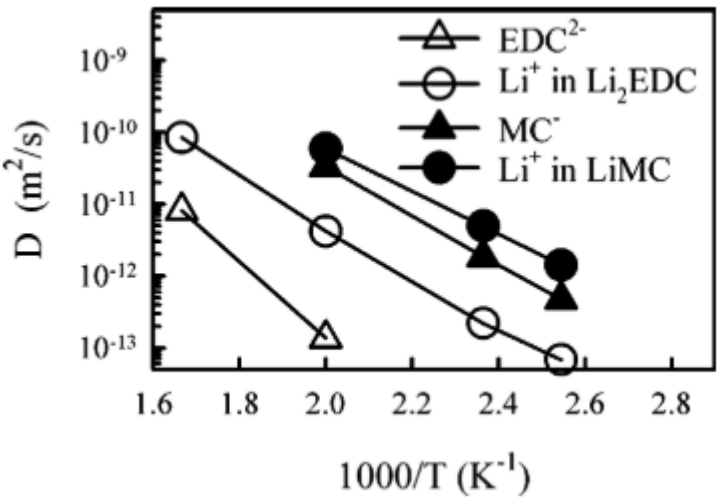


***Figure 8. Dependence of the diffusion coefficient of the electrolyte through the film on temperature [17]***

At room temperature, the diffusion coefficient is $D_{sei} = 1.8 \cdot 10^{-19} \frac{m^2}{s}$.

The values of the SEI molar mass, its density and conductivity are the same in all articles and take the values $M_{sei} = 160\frac{g}{mol}, \rho_{sei} = 1600\frac{kg}{m^3}, \sigma_{sei} = 5 \cdot 10^{-6}\frac{S}{m}$. Data on the conductivity and density of the film depending on temperature are also determined in [17].

# 3. Creating a battery model

## 3.1. Law of conservation of mass in solid body

The concentration of lithium in the solid phase is described by the law

$$\frac{\partial c_s}{\partial t}(r,x,t) = D_s \Delta c_s(r,x,t) = \frac{1}{r^2}\frac{\partial}{\partial r}\left(D_s r^2 \frac{\partial c_s}{\partial r}(r,x,t)\right) \quad (2)$$

Where $D_s$ is the diffusion coefficient of lithium in the solid phase, r is the radial component of the spherical particle. Boundary conditions are determined for lithium flows through the center and out of the particle:

$$\frac{\partial c_s}{\partial r}(r = 0,x,t) = 0$$

Due to symmetry

$$\frac{\partial c_s}{\partial r}(r = R_s,x,t) = -j(x,t)$$

Where $R_s$ is the radius of the particle, $-j(x,t)$ is the flow of lithium from the solid phase to the liquid.

## 3.2. Law of conservation of charge in the solid phase

The potential distribution in the solid phase looks like

$$\nabla \cdot \left(-\sigma^{eff}\nabla\varphi_s(x,t)\right) = -a_{as}Fj(x,t) \quad (3)$$

Where $\sigma^{eff} = \sigma\varepsilon_s^{brug}$ is the effective conductivity in a solid, $\varepsilon_s$ is the volumetric content of the solid phase, brug = 1.5, and $a_{as}$ is the surface area of the solid phase per unit volume.

$$a_{as} = \frac{S_{sphere}}{V_{\text{sphere}}} \cdot \varepsilon_s = \frac{3 \cdot \varepsilon_s}{R_s}$$

Border conditions:

$$\sigma^{eff} \cdot \frac{\partial \varphi_s}{\partial x}(x = 0, t) = -i(t)$$

$$\varphi_s(x = L_{sum}, t) = 0$$

Where $i(t)$ is the external current density, and $L_{sum}$ is the length of the entire electrochemical cell.

## 3.3. Law of conservation of mass in electrolyte

Diffusion in the electrolyte is given by the relation

$$\frac{\partial}{\partial t}\left(\varepsilon_{\mathrm{e}} \cdot c_{\mathrm{e}}(x,t)\right) + \nabla \cdot \left(-D_e^{eff} \cdot \nabla c_e(x,t)\right) = (1 - t_+^0) \cdot a_s \cdot j(x,t) \quad (4)$$

Where $c_{\mathrm{e}}(x,t)$ is the concentration of lithium ions in the electrolyte, $\varepsilon_{\mathrm{e}}$ is the filling fraction of the electrolyte, $D_e^{eff} = D\varepsilon_s^{brug}$ is the effective diffusion coefficient of lithium in the electrolyte, $t_+^0$ is the transport number of lithium ions.

Initial conditions:

$$c_e(x, t = 0) = c_{e0}(x) = c_{e0}$$

Where is the initial concentration of lithium ions in the electrolyte$c_{e0}$

Border conditions:

$$\frac{\partial \mathrm{c}_e}{\partial x}(x = 0, t) = \frac{\partial \mathrm{c}_e}{\partial x}(x = L_{sum}, t) = 0$$

The electrolyte is assumed to be electrically neutral. The number of positive and negative ions is assumed to be the same with identical distribution

$$c_e(x,t) = c_+(x,t) = c_-(x,t) \quad (5)$$

Where $c_+, c_-$ are the concentrations of positive and negative ions in the electrolyte, respectively. Since the total amount of negative ions $PF_6^-$ remains constant without participating in any reactions, the total amount of lithium (the integral of the concentration) in the electrolyte also remains constant.

## 3.4. Law of conservation of charge in electrolyte

Change in potential in the electrolyte:

$$\nabla \cdot \left(-\kappa^{eff} \nabla \varphi_e(x,t) - \kappa_D^{eff} \nabla \ln c_e(x,t)\right) = a_s F j(x,t) \quad (6)$$

Where $\kappa^{eff} = \kappa_e \varepsilon_e^{brug}$ is the specific conductivity of the electrolyte, $\kappa_D = \frac{2\kappa RT}{F}\left(1 + \frac{\partial \ln f_{\pm}}{\partial \ln c_e}\right)(t_+^0 - 1)$ is the coefficient of the term taking into account the electric field arising as a result of ambipolar diffusion, R is the universal gas constant, T is the battery temperature, $F = 96840 \frac{\text{C}}{\text{mol}}$ is Faraday's constant, $f_{\pm}$ is the activity coefficient, $t_+^0$ is the transfer number.

Border conditions:

$$\frac{\partial \varphi_e}{\partial x}(x = 0, t) = \frac{\partial \varphi_e}{\partial x}(x = L_{sum}, t) = 0$$

## 3.5. Butler-Volmer equation

The movement of lithium ions between phases is determined by the Butler-Volmer kinetic equation

$$j(x,t) = \frac{i_0}{F}\left(\exp\left(\frac{(1-\alpha)F}{RT}\eta(x,t)\right) - \exp\left(-\frac{\alpha F}{RT}\eta(x,t)\right)\right) \qquad (7)$$

Where $i_0 = Fk_{0,norm}\left(\frac{c_e}{c_{e0}}\right)^{1-\alpha}\left(\frac{c_{s,max} - c_{s,e}}{c_{s,max}}\right)^{1-\alpha}\left(\frac{c_{s,e}}{c_{s,max}}\right)^{\alpha}$ is the reference current value, $k_{0,norm}$ is the reaction coefficient, $\alpha = 0.5$ is the transfer coefficient, $\eta = (\varphi_s - \varphi_e) - U_{ocp} - dphi$ is overvoltage (deviation of the voltage value in the solid phase from the equilibrium value), $dphi = j \cdot F \cdot \frac{\Delta l_{sei}}{\sigma_{sei}}$ is the voltage drop across the film, $c_{s,e}, c_{s,max}$ – current and maximum value of lithium concentrations in the solid phase, $c_e, c_{e0}$ – current and initial value of lithium concentrations in the electrolyte.

## 3.6. Film growth equations

The side reaction occurs at the interface between the graphite electrode and the electrolyte. The lithium ion reacts with an electrolyte molecule and an electron to form a new compound, the SEI film. The kinetic equation for film growth is similar to the Butler-Volmer equation for transmission lithium into the solid phase, but has several differences: the film reaction proceeds only in the direction of formation (no

destruction) [3], the overvoltage for the film is associated with the reduction potential $U_{sei} = 0.8\,V$ [25]

$$j_{sei}(x,t) = k_{sei\ norm} \cdot \left(\frac{c_{solvent}(x,t)}{c_0} \cdot \frac{c_e(x,t)}{c_{e0}}\right)^{\alpha} \cdot \exp\left(\frac{-\alpha \cdot F \cdot \eta_{sei}(x,t)}{RT}\right) \quad (8)$$

Where $k_{sei\ norm}$ is the film formation reaction coefficient, $c_{solvent}(x,t)$ is the solvent concentration at the surface of the graphite electrode after diffusion through the existing film, and $\eta_{sei} = \eta + U_{ocp} - U_{sei}$ is the overvoltage.

Change in film concentration is related to the reaction flow by the relation

$$j_{sei}(x,t) \cdot a_{as} = \frac{\partial c_{sei}}{\partial t}(x,t) \quad (9)$$

Initial condition for film formation:

$$c_{sei}(x, t=0) = c_{sei\,0}(x) = c_{sei\,0}$$

SEI concentration refers to the concentration of lithium ions that, after a side reaction, is irreversibly transferred to the film. The thickness of this film is related to the concentration by the ratio

$$\Delta l_{sei} = \frac{c_{sei} \cdot M_{sei}}{a_{as} \cdot \rho_{sei}} \quad (10)$$

Now we need to determine the value $c_{solvent}(x,t)$. The derivation of the equation for the solvent concentration near the electrode can be found in Appendix 1. Here we limit ourselves to only the final formula

$$\mathrm{c}_{solvent} = c_0 \cdot \left(1 - Z \cdot \frac{dc_{sei}}{dt} \cdot c_{sei}\right) \quad (11)$$

Where

$$Z = \left(\frac{M_{sei}}{a_{as}}\right)^2 \cdot \frac{1}{\rho_{sei} \cdot M_{solvent} \cdot c_0 \cdot D_{sei}} \quad (12)$$

$M_{sei}, M_{solvent}$ – molar masses of the film and solvent, $\rho_{sei}$ – film density, $D_{sei}$ – diffusion coefficient of solvent molecules through the film.

## 3.7. Derivation of the equation on c_sei

Having compiled a complete system of expressions to describe film growth in section 3.6 (9-12), it is possible to derive a differential equation for the variable $c_{sei}$, which will then be solved in the software package.

$$\frac{\partial c_{sei}}{\partial t} = k_{sei\ norm} \cdot \left(\frac{c_{solvent}(x,t)}{c_0} \cdot \frac{c_e(x,t)}{c_{e0}}\right)^{0.5} \cdot \exp\left(\frac{-0.5 \cdot F \cdot \eta_{sei}(x,t)}{R \cdot T}\right) \cdot a_{as} \cdot \left(1 - Z \cdot c_{sei} \cdot \frac{\partial c_{sei}}{\partial t}\right)^{0.5} \quad (13)$$

In this equation, the derivative of the calculated variable enters both sides with different degrees. In order to write this equation into the COMSOL software package, it must have a certain form, for example $\frac{\partial c_{sei}}{\partial t} = f(c_{sei})$. To obtain an equation in this form, we will resort to additional mathematical transformations

$$\sqsupset F_0(x,t) = k_{sei\ norm} \cdot \left(\frac{c_{solvent}(x,t)}{c_0} \cdot \frac{c_e(x,t)}{c_{e0}}\right)^{0.5} \cdot \exp\left(\frac{-\alpha \cdot F \cdot \eta_{sei}(x,t)}{R \cdot T}\right) \cdot a_{as}$$

Let's divide everything by the sign F0 and solve the equation using a new variable $g = \frac{c_{sei}}{sign(F_0)}$, the derivative of which will be positive. And the value itself also, since $c_{sei}$ is positive. Let's substitute all given expressions into (13) and square it

$$\left(\frac{\partial g}{\partial t}\right)^2 + Z \cdot g \cdot F_0^2 \cdot \frac{\partial g}{\partial t} - F_0^2 = 0$$

Let's find the roots of the equation with respect to the derivative

$$\frac{\partial g}{\partial t} = \frac{1}{2} \cdot \left(-Z \cdot g \cdot F_0^2 \pm sqrt((Z \cdot g \cdot F_0^2)^2 + 4F_0^2)\right)$$

Or

$$\frac{\partial c_{sei}(x,t)}{\partial t} = sign(F_0) \cdot \left(-Z \cdot c_{sei}(x,t) \cdot \frac{F_0^2}{2} + sqrt\left(\left(Z \cdot c_{sei}(x,t) \cdot \frac{F_0^2}{2}\right)^2 + F_0^2\right)\right) \quad (14)$$

# 4. Implementing the COMSOL model

This section discusses in detail the process of creating a model in the COMSOL software package so that readers can repeat the experiments performed and obtain data similar to what will be discussed in the following sections. We will also look at some tricks to solve the system of differential equations (2,3,4,6,14), as well as ways to change various boundary values (for example, constant current to constant voltage) when changing the flag variable.

## 4.1. Setting parameters

***Table 1. Model parameters. Note: technical record, as in the COMSOL program***

| | | |
|---|---|---|
| alpha | 0.5 | Charge transfer coefficient |
| as_neg | 3*(eps_s_neg)/rp_neg | Specific surface area negative |
| as_pos | 3*(eps_s_pos)/rp_pos | Specific surface area positive |
| brug | 1.5 | Bruggeman coefficient |
| brug_sigma | 1 | Bruggeman coefficient for electrode conductivity |
| c_e0 | 1500 [mol/m^3] | Initial electrolyte salt concentration |
| cs_max_neg | 26390 [mol/m^3] | Max solid phase concentration Negative |
| cs_max_pos | 49970 [mol/m^3] | Max solid phase concentration Positive |
| cs_min_pos | 0.5*cs_max_pos | Min solid phase concentration Positive |
| cs0_neg | cs_max_neg*(SoC0_neg)-c_sei_0 | Initial solid phase concentration Negative |
| cs0_pos | cs_max_pos*(1-SoC0/2) | Initial solid phase concentration Positive |
| c_elec | 1500 [mol/m^3] | Electrolyte concentration |
| c_sei_0 | 0[mol/m^3] | Initial SEI concentration |
| D_e | 2.6e-10 [m^2/s] | Salt diffusivity in Electrolyte |
| D_s_neg | 3.9e-14 [m^2/s] | Solid phase Li-diffusivity Negative |
| D_s_pos | 1e-14 [m^2/s] | Solid phase Li-diffusivity Positive |
| D_sei | 1e-20[m^2/s] | SEI diffusion |
| D_sei_elec | M_sei^2/as_neg^2/rho_sei/M_elec/c_elec/Z_ | Electrolyte diffusion through SEI |
| eps_e_pos | 0.315 | Electrolyte phase volume fraction Positive |
| eps_e_sep | 0.724 | Separator porosity |
| eps_s_neg | 0.471 | Solid phase vol-fraction Negative |
| eps_e_neg_init | 0.357 | Electrolyte phase volume fraction Negative |
| eps_s_pos | 0.51 | Solid phase vol-fraction Positive |
| F | F_const | Faraday's constant |
| flag_Li | 1 | Flag for lithium redaction |
| i_app | 13.951 [A/m^2] | Applied current (1C) |

| | | |
|---|---|---|
| kappa_film | 5e-6[S/m] | SEI layer conductivity |
| k_neg_norm | 1.2953e-05 [mol/m^2/s] | Reaction rate coefficient Negative |
| k_pos_norm | 3.1e-4 [mol/m^2/s] | Reaction rate coefficient Positive |
| k_sei_norm0 | 1e-8 [(mol/m^2/s)] | SEI reaction rate coefficient |
| Li_elec_init | c_e0*V_e_init | Initial lithium amount in electrolyte |
| Li_total | 1.26441 [mol/m^2] | Total amount of lithium in the electrodes |
| L_neg | 70e-6 [m] | Length of negative electrode |
| L_pos | 43e-6 [m] | Length of positive electrode |
| L_sep | 76e-6 [m] | Length of separator |
| M_elec | 92[g/mol] | Electrolyte molar mass |
| M_sei | 0.16[kg/mol] | Molar mass of product of side reaction |
| Q_neg | F*L_neg*eps_s_neg*cs_max_neg | Capacity of the negative electrode |
| Q_pos | F*L_pos*eps_s_pos*(cs_max_pos-cs_min_pos) | Capacity of the positive electrode |
| R | R_const | Gas constant |
| rho_sei0 | 1.6e3[kg/m^3] | Density of product of side reaction |
| rp_neg | 12.5e-6 [m] | Particle radius Negative |
| rp_pos | 4.25e-6 [m] | Particle radius Positive |
| sigma_neg | 100 [S/m] | Solid phase conductivity Negative |
| sigma_pos | 6.9 [S/m] | Solid phase conductivity Positive |
| SoC0 | 0.1 | Initial state of charge Positive |
| SoC0_neg | 0.25671 | Initial state of charge Negative |
| time_accelerate | 1 | Time acceleration |
| t_plus | 0.363 | Cationic transport number |
| t1 | 3151[s] | Stoppage time |
| U_stop | 4.1785[V] | Stoppage voltage |
| U_sei | 0.8[V] | SEI decomposition potential |
| V_pos | L_pos*eps_s_pos | Volume of the solid phase of the electrode Positive |
| V_neg | L_neg*eps_s_neg | Volume of the solid phase of the electrode Negative |
| V_e_init | L_pos*eps_e_pos + L_sep*eps_e_sep + L_neg*eps_e_neg_init | Electrolyte volume |
| SoC_neg_stop | (Li_total - cs_max_pos*V_pos*(1 - SoC_pos_stop/2))/cs_max_neg/V_neg | Stoppage negative State of Charge |
| SoC_pos_stop | 0.95 | Stoppage positive State of Charge |
| Z_0 | 50[m^6*s/mol^2] | Z constant |
| flag_current | 1 | Flag whether current flows |
| T_ref0 | 25 [degC] | Reference temperature |

First of all, before modeling a problem, it is necessary to determine a complete set of parameters describing the state of the system. They are shown in Table 1. It is

not always possible to find exact parameter values for each battery, so it was necessary to check with what accuracy certain parameters need to be measured.

Separately, it is worth noting that when analyzing the model, the importance of smoothness of the graph $U_{ocp}$ was revealed, therefore it is the data approximation equation in Figure 4 that is given, and not a table of values. When the derivative $\frac{\partial U_{ocp}(SoC)}{\partial SoC}$, where $SoC$ is the degree of charge of the battery (Figure 9a), was broken, sharp potential jumps appeared along the length of the battery on adjacent grid elements (Figure 9b).

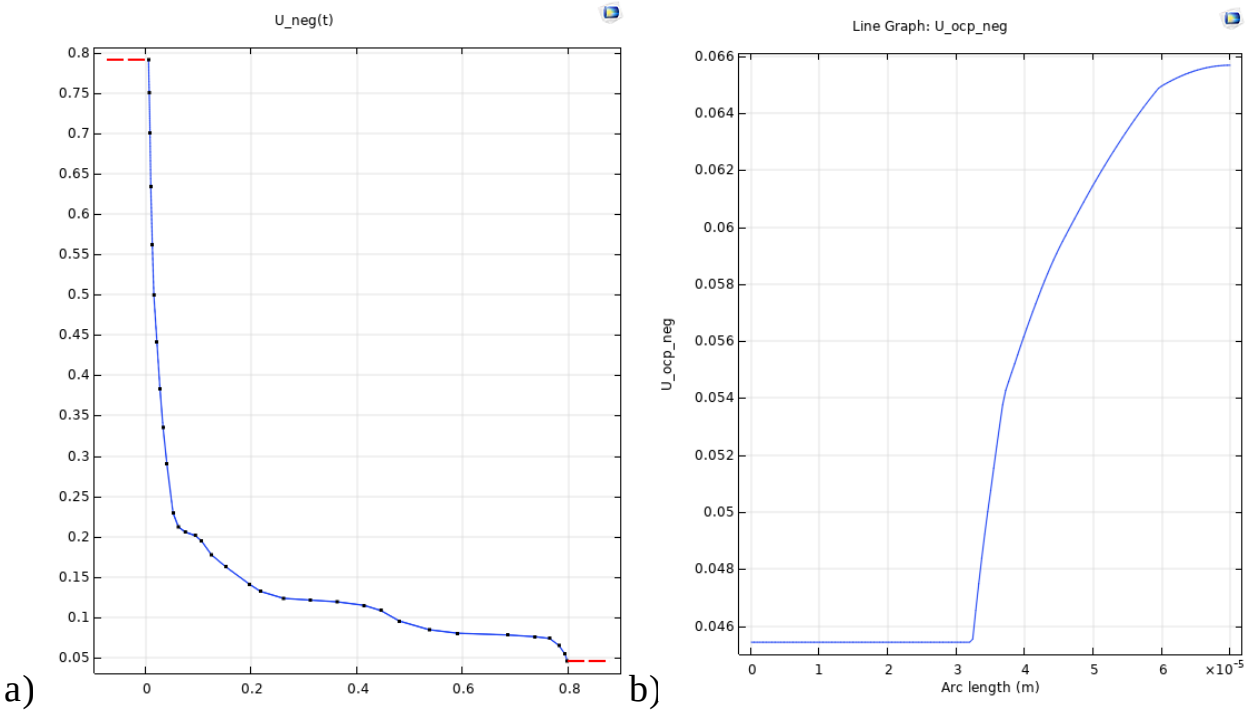


***Figure 9. a) Graph of open circuit voltage leading to b) Sharp voltage surges along the electrode boundary***

## 4.2. Geometry

The basic geometry of the model consists of 3 parts: positive electrode, negative electrode and separator (Figure 10a). An additional description of the distribution process of lithium-ion concentration inside solid particles is carried out in pseudo-space. Accordingly, an additional component with two-dimensional geometry is used for this (Figure 10b). Each particle corresponds to a segment parallel to the y-axis, along which diffusion occurs.

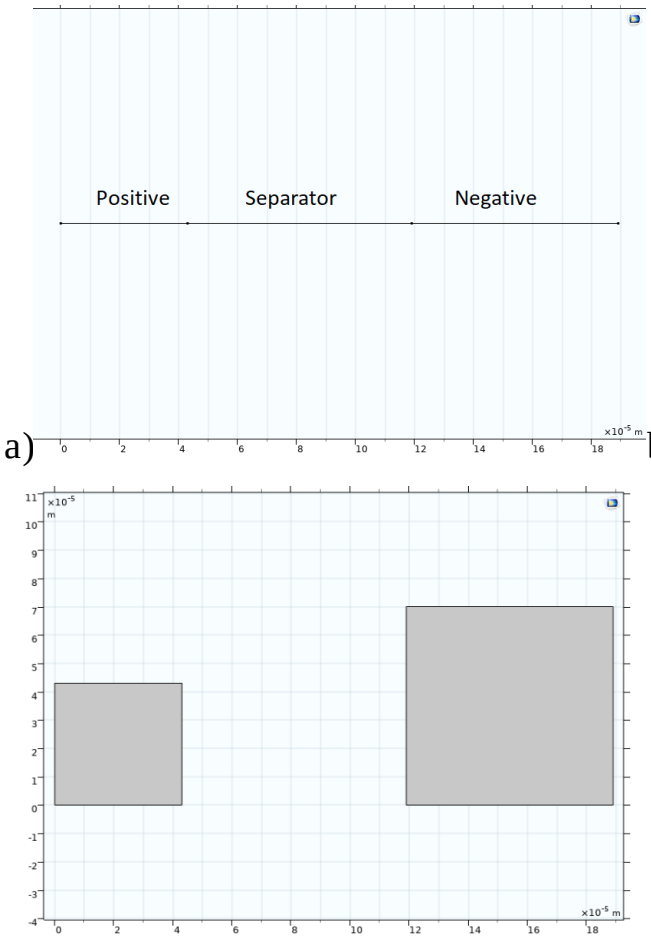


***Figure 10. a) Basic geometry, b) Pseudospace.***

## 4.3. System of equations

To describe the system of equations, we will use the analogy of writing polymorphic code. So, the equations will be specified at the level of abstraction of behavior, and their specific implementation will be different in each electrode. This was done mainly to avoid cluttering the model and to solve the system with fewer equations. Thus, the equations will be written for the maximum total number of domains, and the coefficient values will be specified in the "Variables" section for each electrode separately. Tables of variable values are presented in tables 2,3,4.

***Table 2. COMSOL Positive Electrode Variables***

| | | |
|---|---|---|
| as | as_pos | Specific surface area |
| cse | pseudo_dim.pos_cse(c_s) | Average lithium concentration in electrode |
| D_e_eff | (D_e+D_eT*(T_ref-T_ref0))*eps_e^brug | Effective salt diffusivity in electrolyte |
| eps_e | eps_e_pos | Electrolyte phase volume fraction |
| eta | phi_s-phi_e-U_ocp_pos | Overpotential |

| | | |
|---|---|---|
| j0 | k_pos_norm_eff*abs((cs_max_pos-cse)/cs_max_pos)^(1-alpha)*abs(cse/cs_max_pos)^alpha*abs(c_e/c_e0)^(1-alpha) | Lithium flow between solid and liquid phase |
| j_ | j0*(exp((1-alpha)*F*eta/(R*T_ref))-exp(-alpha*F*eta/(R*T_ref))) | The rate of lithium movement between the solid and electrolyte |
| kappa_eff | (kappa(0.001*c_e) + kappaT*(T_ref - T_ref0))*eps_e_pos^brug | Effective electrolyte conductivity |
| sigma_eff | sigma*eps_s_pos^brug_sigma | Effective electrode conductivity, |
| sigma | sigma_pos | Electrode conductivity |
| kappa_D | 2*R*T_ref/F*(1-t_plus) | Junction potential coefficient |
| k_pos_norm_eff | k_pos_norm*exp(Ear_p/R*(1/298.15 [K] - 1 /T_ref)) | k_pos_norm at current temperature |
| U_ocp_pos | U_pos(cse/cs_max_pos) + dUdT_pos(cse/cs_max_pos)*(T_ref - T_ref0) | U_ocp potential at current temperature |

***Table 3: Variables Defined in COMSOL for the Negative Electrode***

| | | |
|---|---|---|
| as | as_neg | Specific surface area |
| cse | pseudo_dim.neg_cse(c_s) | Average lithium concentration in electrode |
| dphi | j_*F*thick_sei/kappa_film | Potential on SEI |
| D_e_eff | (D_e +D_eT*(T_ref - T_ref0))*eps_e^brug | Effective salt diffusivity in electrolyte |
| eps_e | eps_e_neg | Electrolyte phase volume fraction |
| eta_sei_back | phi_s-phi_e-U_sei-dphi | |
| eta_0_neg | eta-(phi_s-phi_e-U_ocp_neg-dphi) | Additional variable |
| F01 | k_sei_norm*as*abs(c_e/c_e0)^(1-alpha)*abs(c_elec/c_elec)^(1-alpha)*exp_sei | F in (14) |
| j0 | k_neg_norm_eff*abs((cs_max_neg-cse)/cs_max_neg)^(1-alpha)*abs(cse/cs_max_neg)^alpha*abs(c_e/c_e0)^(1-alpha) | Lithium flow between solid and liquid phase |
| j_ | j0*(exp((1-alpha)*F*eta/(R*T_ref))-exp(-alpha*F*eta/(R*T_ref))) | The rate of lithium movement between the solid and electrolyte |
| kappa_eff | (kappa(0.001*c_e) + kappaT*(T_ref - T_ref0))*eps_e_neg^brug | Effective electrolyte conductivity |
| sigma | sigma_neg | Electrode conductivity |
| sigma_eff | sigma*eps_s_neg^brug_sigma | Effective electrode conductivity, |
| sign | sign(F01) | |
| source1 | siggn*(sqrt(F01^2+(1/2*Z_*c_sei*F01^2)^2)*sign_func-1/2*Z_*c_sei*F01^2) | Source in (14) |
| source2 | c_seit/as*eps_s_neg | Lithium decrease coefficient |
| thick_sei | (c_sei)*M_sei/rho_sei/as | SEI thickness |
| kappa_D | 2*R*T_ref/F*(1-t_plus) | Junction potential coefficient |
| k_neg_norm_eff | k_neg_norm*exp(Ear_n/R*(1/298.15 [K] - 1 /T_ref)) | Effective k_neg_norm |

| | | |
|---|---|---|
| U_ocp_neg | U_neg(cse/cs_max_neg)+ dUdT_neg(cse/cs_max_neg)*(T_ref - T_ref0) | Open circuit potential for electrode |
| eta_sei | phi_s-phi_e-U_ocp_neg-dphi | Overpotential for c_sei variable |
| exp_sei | exp(-alpha*F*(U_ocp_neg+eta-U_sei)/(R*T_ref)) | Part of F variable |

***Table 4: COMSOL Separator Variables***

| | | |
|---|---|---|
| as | 0 [m^-1] | Specific surface area |
| D_e_eff | (D_e +D_eT*(T_ref - T_ref0))*eps_e^brug | Effective salt diffusivity in electrolyte |
| eps_e | eps_e_sep | Separator porosity |
| j_ | 0 [mol/m^2/s] | The rate of lithium movement between the solid and electrolyte |
| kappa_eff | (kappa(0.001*c_e) + kappaT*(T_ref - T_ref0))*eps_e_sep^brug | Effective electrolyte conductivity |
| kappa_D | 2*R*T_ref/F*(1-t_plus) | Junction potential coefficient |

## 4.4. Basic Equations

The governing equations were written using the General form of Differential Equations (General form PDE) in COMSOL. In the main component, equations were solved for the laws of charge conservation for the solid (3) and liquid phases (6), and the law of conservation of electrolyte mass (4).The law of conservation of mass in the solid phase (2) was solved in pseudo-space. The connection between the components was specified through Linear Extrusion operators for each electrode separately. Screenshots of setting equations from the COMSOL program are presented in Figures 11-14.

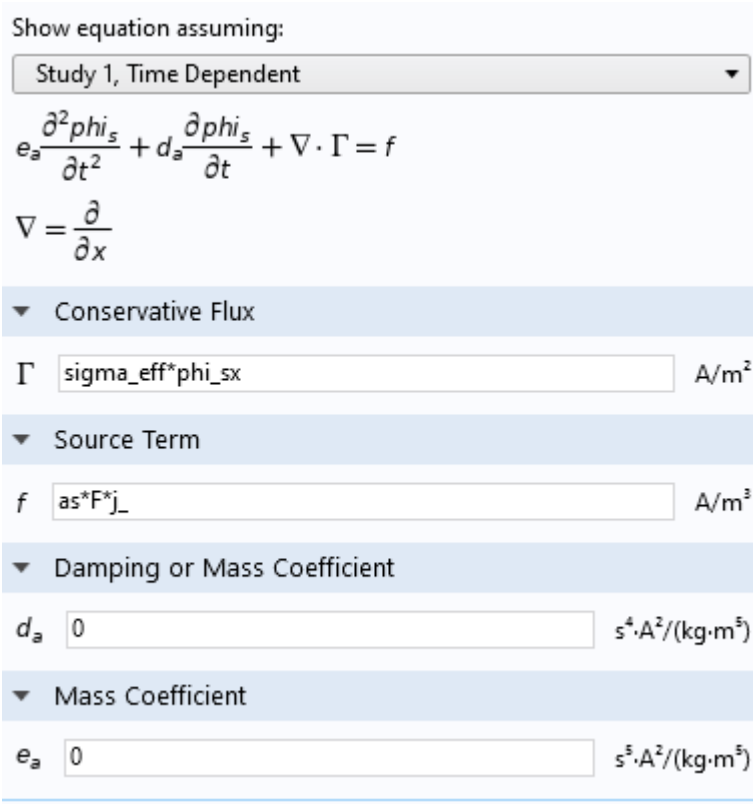


***Figure 11. Screenshot from the COMSOL program with the settings of the General form PDE module, with the help of which the charge conservation law was calculated in the solid phase (3).***

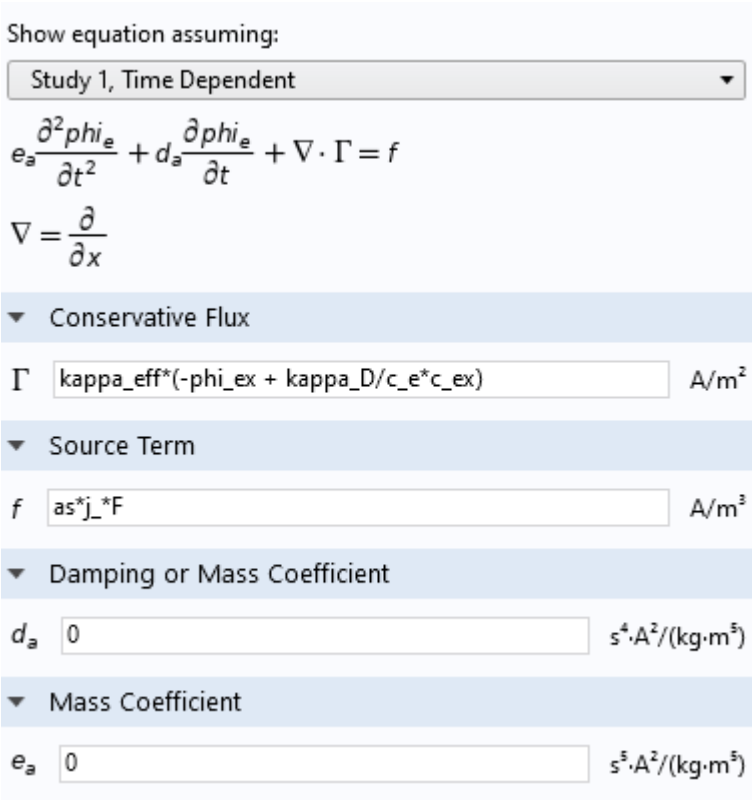


***Figure 12 Screenshot from the COMSOL program with the settings of the General form PDE module, with the help of which the law of conservation of charge in the electrolyte (6) was calculated.***

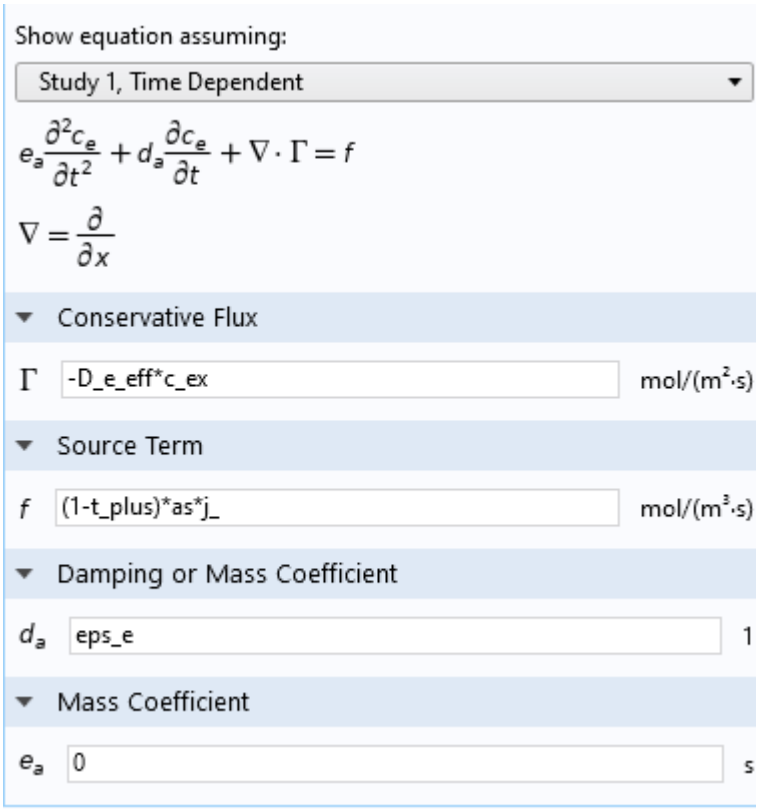


***Figure 13. Screenshot from the COMSOL program with the settings of the General form PDE module, which was used to calculate the diffusion of lithium ions in the electrolyte (4).***

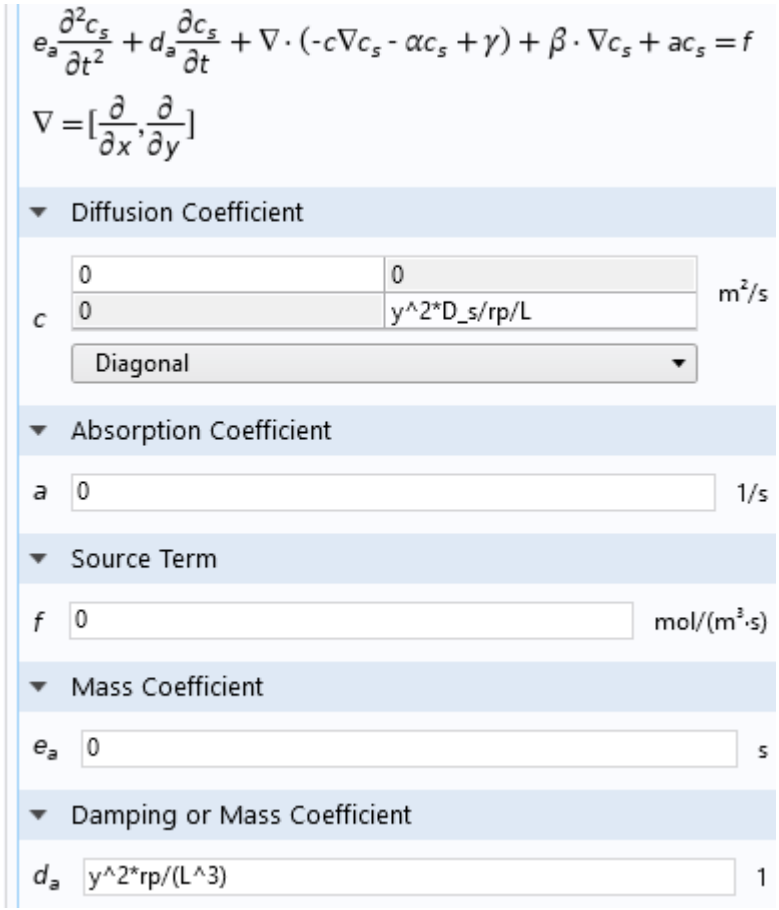


***Figure 14. Screenshot from the COMSOL program with the settings of the General form PDE module, which was used to calculate the diffusion of lithium ions in the solid phase (2).***

## 4.5. Equation on SEI

To describe the equation on SEI, the coefficient form module (Coefficient form PDE) was used. The basis of the equation for SEI is taken from equation (14), but with some additions, which will be discussed later.

The resulting equation for SEI is:

$$\frac{eps\ s\ neg}{time\ accelerat} \cdot \frac{\partial c_{sei}}{\partial t} - D_{sei} \cdot \Delta c_{sei} = source_1$$

Where $time\ accelerat$ is the time "acceleration" coefficient for the growth of the film layer, and $D_{sei}$ is the diffusion coefficient of molecules films from one particle to another (needed to smooth out machine calculation errors).

### 4.5.1. Adding a diffusion contribution

Since the growth of the SEI layer occurs at each point of the negative electrode independently, the error that appears during the solution tends to accumulate and lead to strong uneven growth of the SEI layer (Figure 15) along the spatial coordinate.

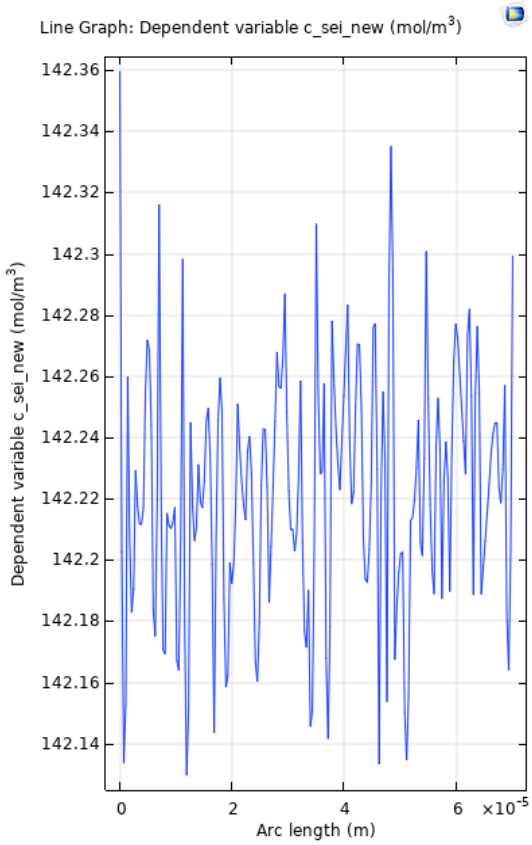

***Figure 15. Film concentration distribution along the negative without spatial diffusion***

This error with increasing layer size leads to inaccuracies caused by the mathematical error of the solution and the inability to achieve the specified accuracy during calculation. To increase stability, it is necessary to connect solutions at adjacent lattice nodes. For this purpose, an additional diffusion coefficient of the SEI layer along the real space coordinate is introduced. Its value should have virtually no effect on the course of the solution, but would have a value sufficient to redistribute SEI between neighboring lattice nodes during the characteristic operating time of the battery. Then:

$$D_{sei} = \frac{a}{t^2} = \frac{1\ \text{мкм}}{(5\ \text{лет})^2} \sim 1e-20\ \text{м}^2/c$$

### 4.5.2. Accelerated film layer growth

Since the growth of the SEI layer is a very long process, the task of simulating it during the charge/discharge process takes a long time (1 hour for 20 cycles (one charge/discharge cycle – 2 hours of virtual time)). Especially to solve such problems and speed up the calculation time with a decrease in the number of cycles, it was decided to artificially accelerate the growth of the layer. To do this, an additional factor was introduced in the existing equation in front of time.

Thus, if a certain amount of time passed for a regular model, then for SEI this time became time_accelerat times longer.

The correct operation of the accelerated layer can be verified using characteristic times (several years) of battery operation in all operating modes. For now, we will limit ourselves to the mode without connection to an external circuit.

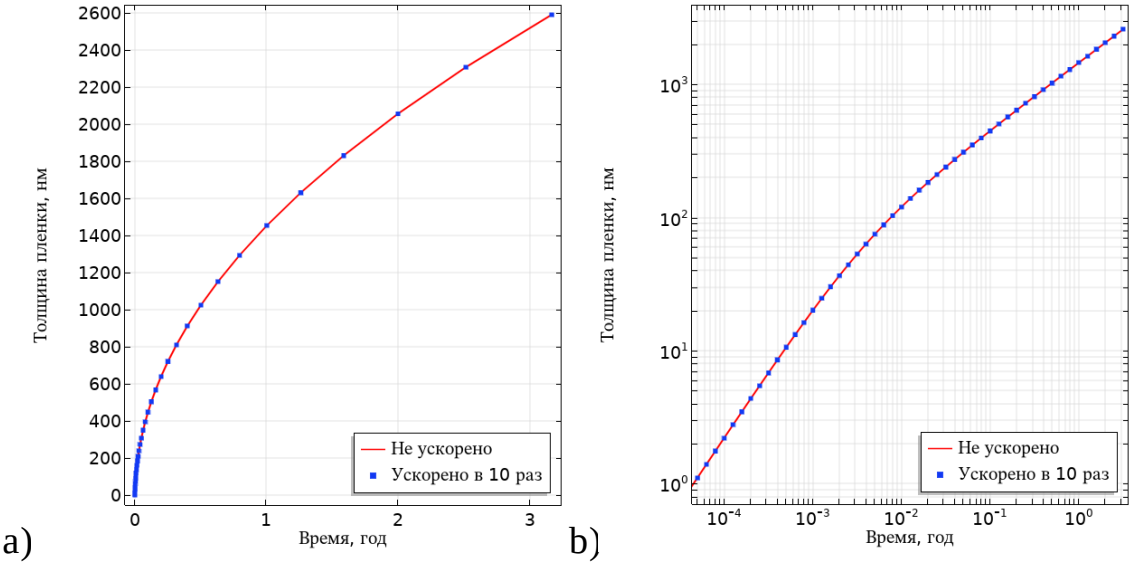


***Figure 16. Graph of film thickness versus time with and without acceleration a) On a regular scale b) On a logarithmic scale***

Figure 16 shows this relationship. Based on this, you can make sure that adding acceleration to the growth of the layer does not affect the trend in the autonomous existence of the battery.

### 4.5.3. Implementation in COMSOL

Solver module settings are presented in Figure 17.

$$e_a\frac{\partial^2 c_s ei}{\partial t^2} + d_a\frac{\partial c_s ei}{\partial t} + \nabla\cdot(-c\nabla c_s ei - \alpha c_s ei + \gamma) + \beta\cdot\nabla c_s ei + a c_s ei = f$$

$$\nabla = \frac{\partial}{\partial x}$$

Diffusion Coefficient

| | | |
|---|---|---|
| $c$ | D_sei | $m^2/s$ |

Absorption Coefficient

| | | |
|---|---|---|
| $a$ | 0 | 1/s |

Source Term

| | | |
|---|---|---|
| $f$ | source1 | $mol/(m^3 \cdot s)$ |

Mass Coefficient

| | | |
|---|---|---|
| $e_a$ | 0 | s |

Damping or Mass Coefficient

| | | |
|---|---|---|
| $d_a$ | eps_s_neg*time_accelerat | 1 |

***Figure 17. Screenshot from the COMSOL program with the settings of the Coefficient form PDE module, which was used to calculate the film growth equation(14)***

It is important to note once again that this implementation is based on a physical model of film growth, supplemented with terms that have little effect on the solution, thanks to which it is possible to speed up both the program and avoid the accumulation of computational errors.

## 4.6. Overvoltage Equation

Solving the existing system after adding an equation for film growth leads to an error in specifying the variables, because an algebraic equation appeared on them.To solve this problem, the following method was found. The expression for the variable in the region of the negative electrode was initially as follows:$eta$

$$eta = phi_s - phi_e - U_{ocp\,neg} - dphi$$

This expression was replaced by a search for its discrepancy. Namely

$$eta\ 0\ neg = eta - \left(phi_s - phi_e - U_{ocp\,neg} - dphi\right)$$

And the equation

$$eta\ 0\ neg = 0$$

After these manipulations, such an error did not occur.

## 4.7. Various charging types. Events module

At this stage, direct current charging is implemented, however, in real models, sequential direct current charging is implemented, which turns into constant voltage charging upon reaching a certain value $U_{stop}$. It is also possible to transition from charging with constant current to discharging (the current changes sign) and cessation of charging followed by relaxation ($i = 0$).

In total, 4 ways of interaction of the battery with an external circuit can be considered:

- DC charging and relaxation
- DC charge/discharge cycles
- Charging with constant current and then constant voltage
- Relaxation

To simulate all possible types of charging within one model, the event handler was used in conjunction with a module for solving a homogeneous differential equation.

In the event module, you need to create variables ($stop\ cond1$ and $stop\ cond2$) in the Indicator State. The first variable corresponds to the event of reaching the maximum voltage, the second - to the minimum. Then, in Discrete state, set the names and initial values of the variables that will change when an event occurs. In our case this is $current\ sign$ and $flag\ temp$. And then in the Implicit Event, register the change in parameters when the conditions $stop\ cond1 > 0$ and $stop\ cond2 < 0$ are reached.

To implement a constant voltage, you cannot simply set a new condition on the boundary; it is better to use an implicit expression for the current, the value of which would be such as to maintain a constant voltage in the battery. This can be realized using an ODE module for the external circuit current.

The equation for Current is as follows:

$$abs(current\ sign) \cdot \frac{current\ sign \cdot Current + flag\ temp \cdot i_{app}}{i_{app}} + \left(1 - abs(current\ sign)\right) \cdot \frac{U_{cell} - U_{stop}}{U_{stop}} = 0$$

Where $current\ sign$ and $flag\ temp$ are event indicators, $i_{app}$ – charging current, $U_{cell}$ – current battery voltage, $U_{stop}$ – stop voltage.

The indicator values for the implementation of the modes are presented in Table 5.

***Table 5. Indicators to check for correctness***

| Charging mode | $current\ sign$ | $flag\ temp$ |
|---|---|---|
| DC charging | 1 | 1 |
| DC discharge | -1 | 1 |
| Constant voltage charging | 0 | 0 |
| Relaxation | 1 | 0 |

Thus, all 4 operating modes were created.

# 5. Analysis of the received data

## 5.1. Analysis of characteristic distributions

First of all, it is necessary to check the correctness of the model by considering the distribution of calculated values. Consider the concentration distribution

To begin with, let us analyze the characteristic concentration distributions.

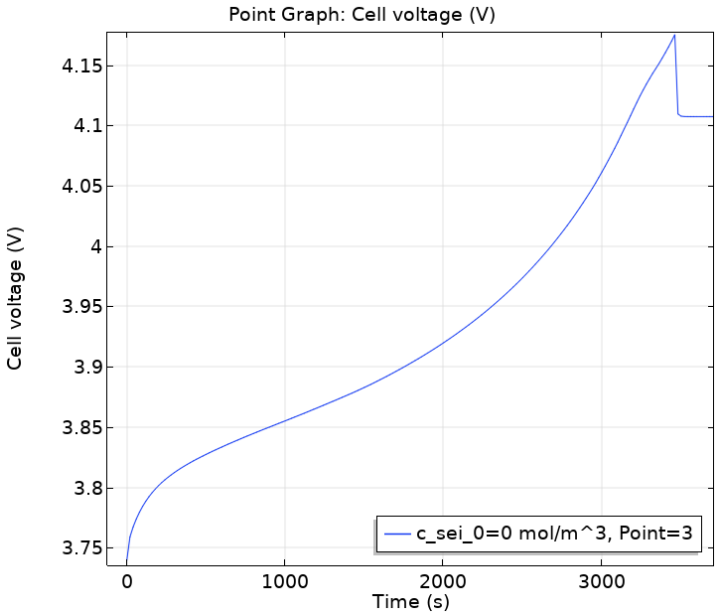


***Figure 18. Oscillogram of DC charging followed by relaxation***

Let's choose a charge cycle - charge with direct current (oscillogram in Figure 18) and see how the distribution of concentration on the positive electrode changes (on the negative everything will be similar)

a)

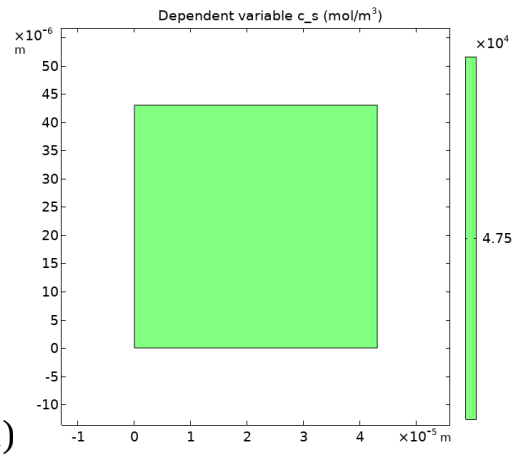


b)

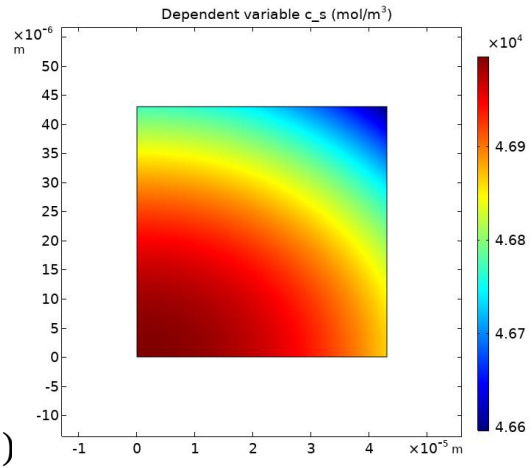

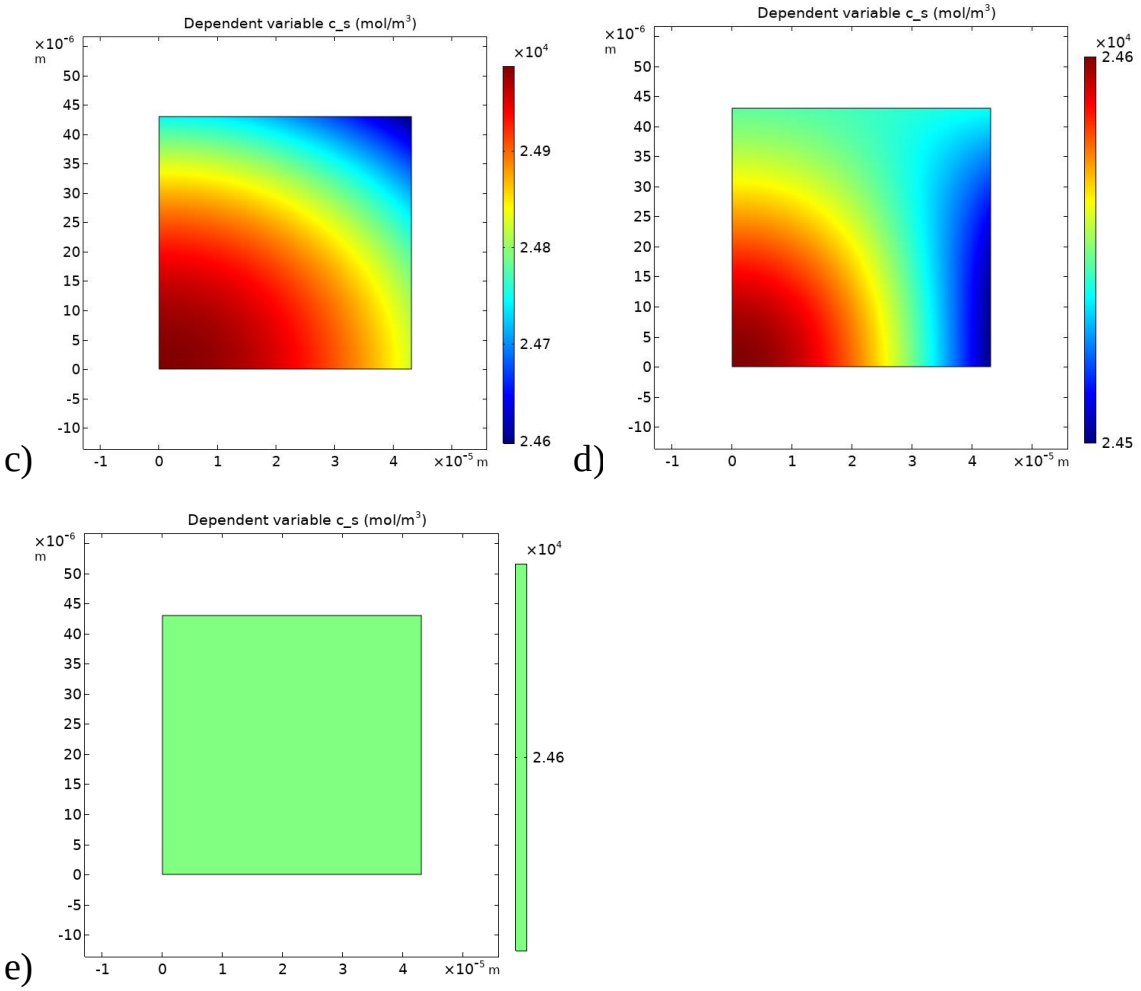


***Figure 19. Concentration distribution at time point A) 1s b) 100 s c) 3440 (before charging stops) d) 3500 (transient process) e) 3600 (establishing equilibrium)***

At the initial moment, the concentration on the entire solid electrode is identical (Figure 19a). When a direct current is applied, lithium begins to leave the solid particle, moving along the y-axis. Moreover, the further a solid particle is from the collector, the more lithium comes out of it (Figure 19b). This is due to the large value of overvoltage when moving away from the edge of the battery (Figure 20).

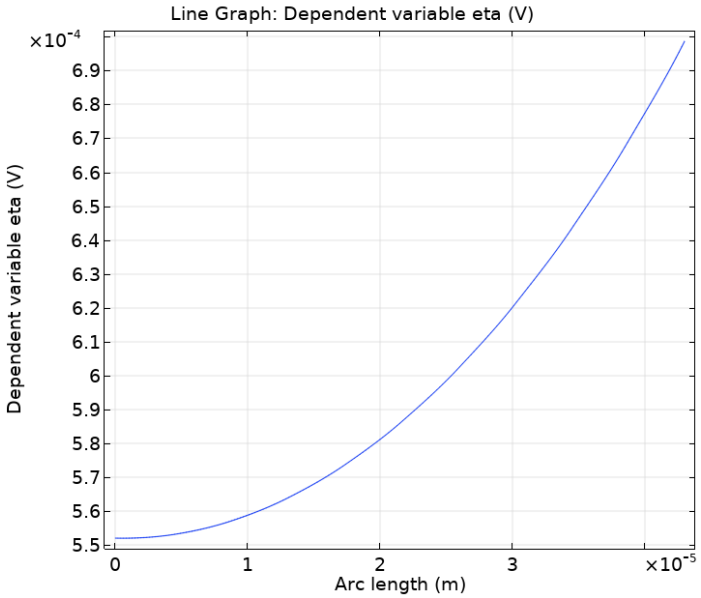


***Figure 20. Overvoltage distribution along the positive electrode at 100 seconds***

The characteristic type of distribution remains until the very end of charging (Figure 19c). After the charging stops, the relaxation process begins. Lithium ions diffuse into the solid particles. The transition process is presented in Figure 19d. After relaxation, the lithium concentration became constant along the entire segment on the y axis. Diffusion does not occur along the x axis, however, with some accuracy (up to 4 significant figures), the difference in concentrations can be considered insignificant (Figure 19e).

Let us now move from the analysis of characteristic distributions in which the correct operation of the model was checked to the study of the obtained data.

## 5.2. The importance of taking into account volume reduction during SEI layer growth

As the film thickness on the negative electrode increases, the volume occupied by the electrolyte decreases.

Consider the radius of the ball

$$\mathrm{r}p \rightarrow rp + \Delta l_{sei}$$

$$\frac{4}{3} pi \cdot ((rp + \Delta l_{sei})^3 - rp^3) \cdot N = \Delta V_{sph} = -\Delta V_{elec}$$

The change in the volume of the electrolyte is determined precisely by the increase in the thickness of the SEI layer

$$\frac{V_{elec}}{V_{sum}} = \frac{V_{elec0}}{V_{sum}} - \frac{\Delta V_{elec}}{V_{sum}} = \frac{V_{elec0}}{V_{sum}} - \frac{\frac{4}{3}pi \cdot rp^3 \cdot N}{V_{sum}} \cdot \left(\left(\frac{rp + \Delta l_{sei}}{rp}\right)^3 - 1\right)$$

Or if we translate everything into relative volume values:

$$eps\ e\ neg = eps\ e\ neg_{init} - eps\ s\ neg \cdot \left(\left(\frac{rp + \Delta l_{sei}}{rp}\right)^3 - 1\right)$$

Also, when the volume fraction of the electrolyte changes, its concentration remains unchanged. However, from a physics point of view, the number of lithium ions (and the number of negative ions) in the electrolyte must remain constant. To realize this effect, it is necessary to add a lithium source to the area where the amount of lithium decreases. The easiest way to implement it is by adding as a source Li the difference between the initial and final values, added at a small point in time. Let's neglect the distribution of the drop in the amount of lithium along the coordinate, because this is an effect of a lower order, and set a source distributed over the entire negative electrode.

During the calculation of the problem, the following graphs were obtained of the dependence of the decrease in the filling of the negative electrode with electrolyte depending on the film thickness.

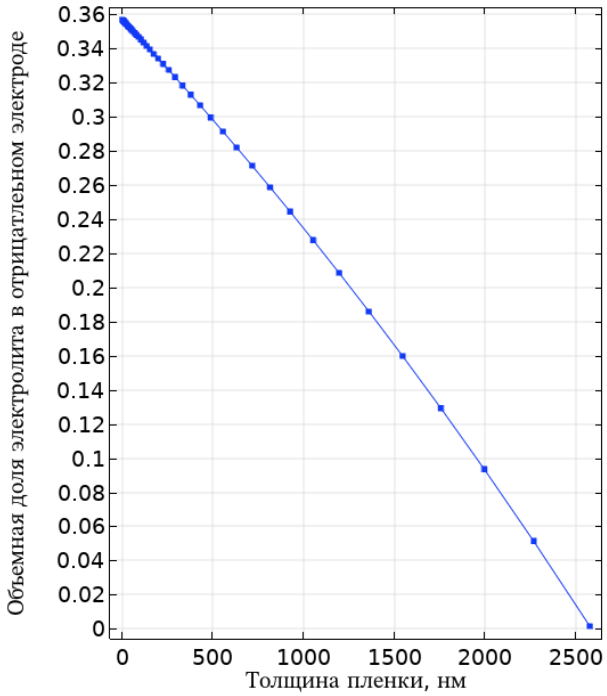


***Figure 21. Dependence of the electrolyte fraction in the negative electrode on the film thickness.***

The maximum film thickness can be determined based on the characteristic values of potential drops and charging currents.

$$\Delta l_{sei} = \frac{\Delta U \cdot \sigma}{j \cdot F} = \frac{0.6\,\text{В} \cdot 5 \cdot 10^{-6}\,\frac{1}{m \cdot Ohm}}{1.8\,\frac{\text{А}}{m^2}} = 1600\,nm$$

At a given value of film thickness, based on Figure 21, the volume fraction of the electrolyte in the negative electrode decreases to 0.15. Let us compare the growth dynamics of the film layer at given values of the electrolyte filling fractions.

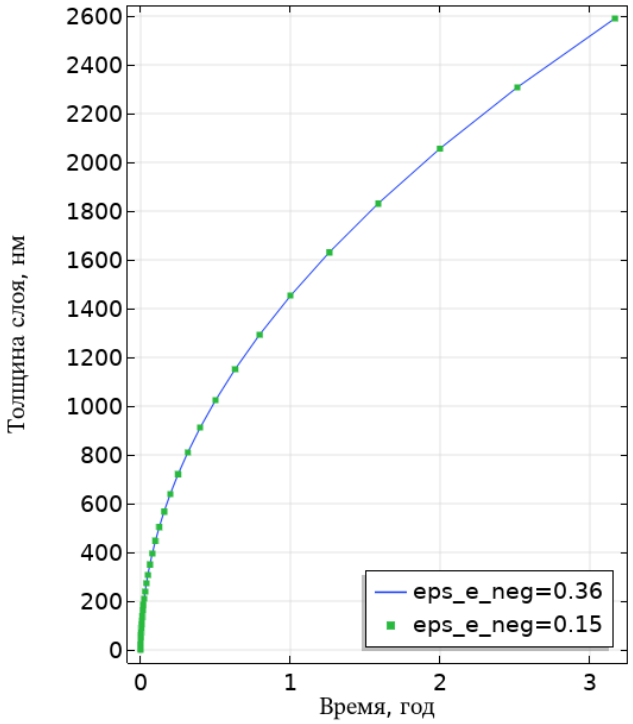


***Figure 22. Dependence of film thickness on time for different values of the degree of filling of the negative electrode with electrolyte***

Film growth shows similar dynamics, which means that the effect of changes in the volume fraction of the electrolyte can be ignored when the film layer thickness increases to at least 1600 nm. However, based on Figure 22, the thickness of the layer increases over several years to slightly more than 1600 nm. This raises questions about setting parameters, which will be discussed in the following sections.

We will also check how changing this parameter affects the voltage oscillogram. For definiteness, let's take a graph of a charge with constant current, turning into a charge with constant voltage (Figure 23).

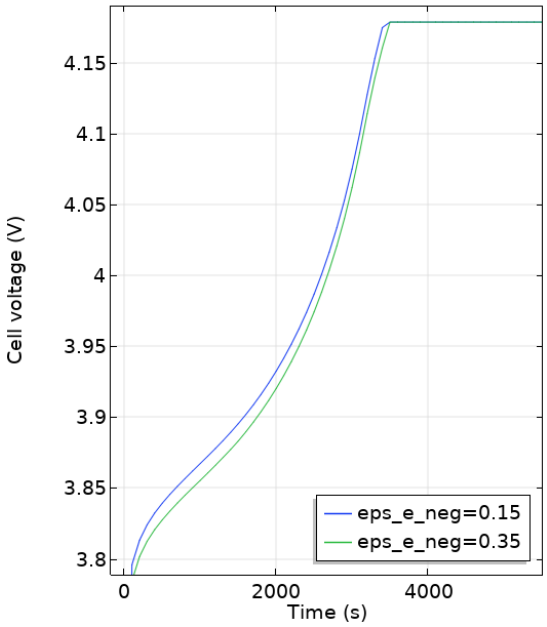


***Figure 23. Oscillogram of charging with constant current and voltage for various values of the degree of filling of the negative electrode with electrolyte***

Even for critical values of the parameter, the difference in the oscillograms is insignificant. The norm in space L1 (maximum deviation) does not exceed 0.03 V, and the charging time to maximum voltage differs by 100 seconds (2% of the total charging time).

From this analysis we can conclude that changing the degree of filling of the negative electrode with electrolyte does not significantly affect film growth and the voltage oscillogram. This means that when solving problems, this effect can be neglected, thereby simplifying the existing model.

## 5.3. Increase in SEI with different charging cycles

This section will review all previously defined charging cycles, and also explore the differences that determine them. Before studying operating modes, it was not clear how quickly the SEI layer grows, whether a specific operating mode greatly affects its growth, and whether the operating mode can be neglected by reducing the calculation time (by simplifying the model or adding time acceleration). This section will also show that the growth rate of the film depends not only on its characteristic properties, such as the reaction coefficient and diffusion coefficient, but also on the state of charge of the battery.

$$SoC = \frac{c - c_{min}}{c_{max} - c_{min}}$$

Where are $c_{max}, c_{min}, c$ the maximum, minimum and current lithium concentrations in the electrode.

A detailed implementation of the various charging cycles is given in Part 4.7.

### 5.3.1. Battery out of circuit

The overvoltage $\eta_{sei} = (\varphi_s - \varphi_e) - U_{sei} - dphi = \eta + U_{ocp}(SoC_{pos}, SoC_{neg})$ involved in the film growth equation is an implicit function of the state of charge of each electrode. Thus, an assumption arises that by changing the degree of charge of the electrodes, it is possible to influence the film growth rate. Let us check this assumption by separately varying the degree of charge of the positive and negative electrodes and comparing the film growth rates in the absence of current.

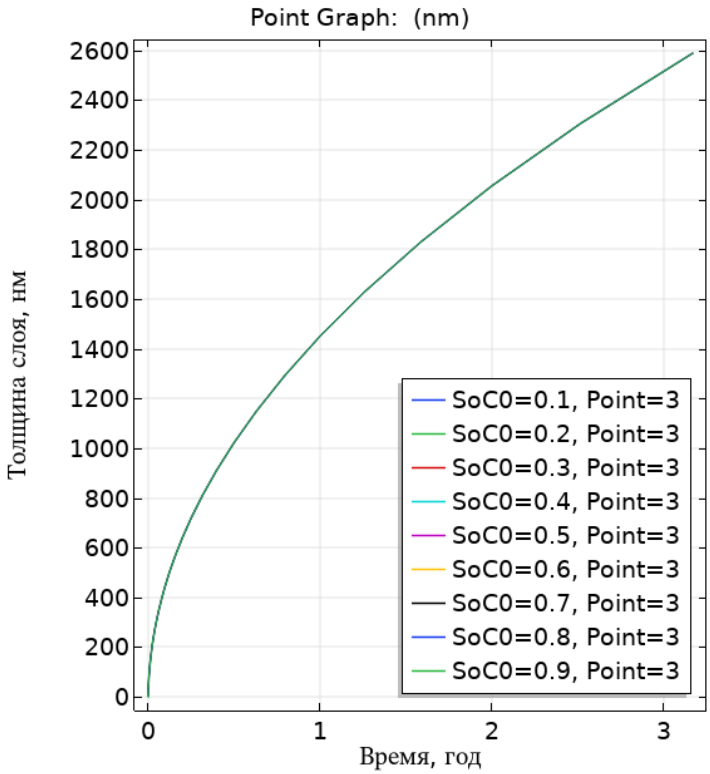


***Figure 24. Graph of film thickness versus time for various degrees of charge of the positive electrode***

Visible difference depending on the state of charge for the positive electrode is not observed in Figure 24. This means that if there are any mechanisms due to which the battery degrades faster, they are located in the area of the negative electrode.

Let us determine the dependence of the growth rate of the film layer on the amount of excess lithium stored in the carbon electrode (see paragraph “Capacity drop”).

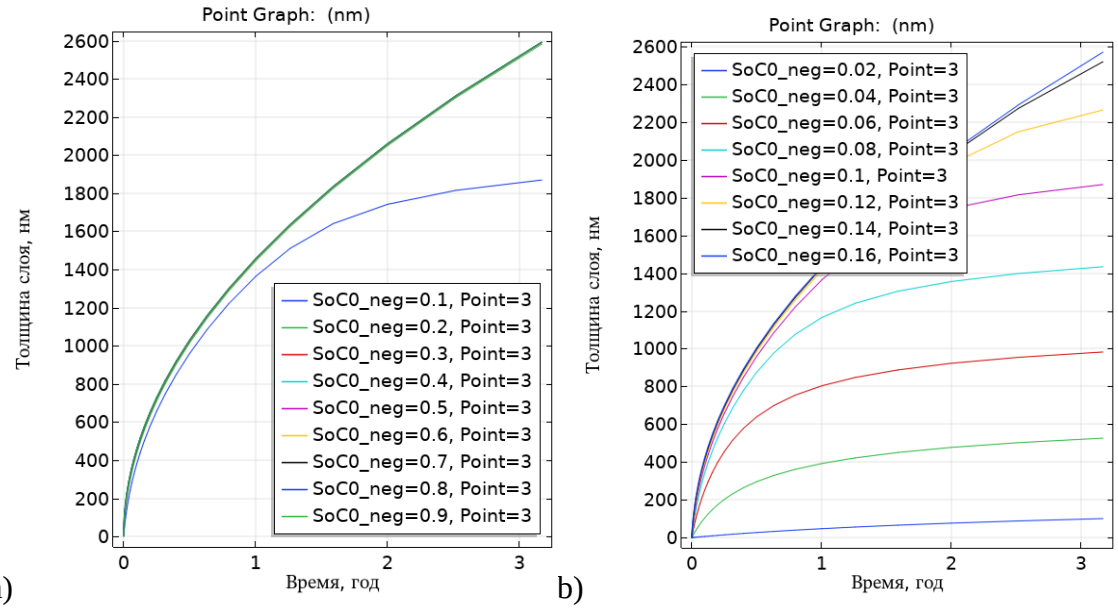


a) b)

***Figure 25. Film thickness versus time plot for different SoCs on the negative electrode. A) rough variation b) fine variation***

Starting from a certain point in time (defined for each SoC_neg0), the growth of SEI begins to slow down in comparison with curves corresponding to large values of SoC_neg0 (Figure 25). Even though the battery is disconnected from the external circuit, the amount of lithium in the electrodes decreases. This is due to a side reaction that occurs on the negative electrode, during which a film is formed. The total amount of lithium in the model remains constant, but some of it is spent on film formation, reducing the amount of lithium in the electrodes and SoC_neg in particular. The dynamics of changes in the degree of charge of the negative electrode over time under different initial conditions are shown in Figure 26.

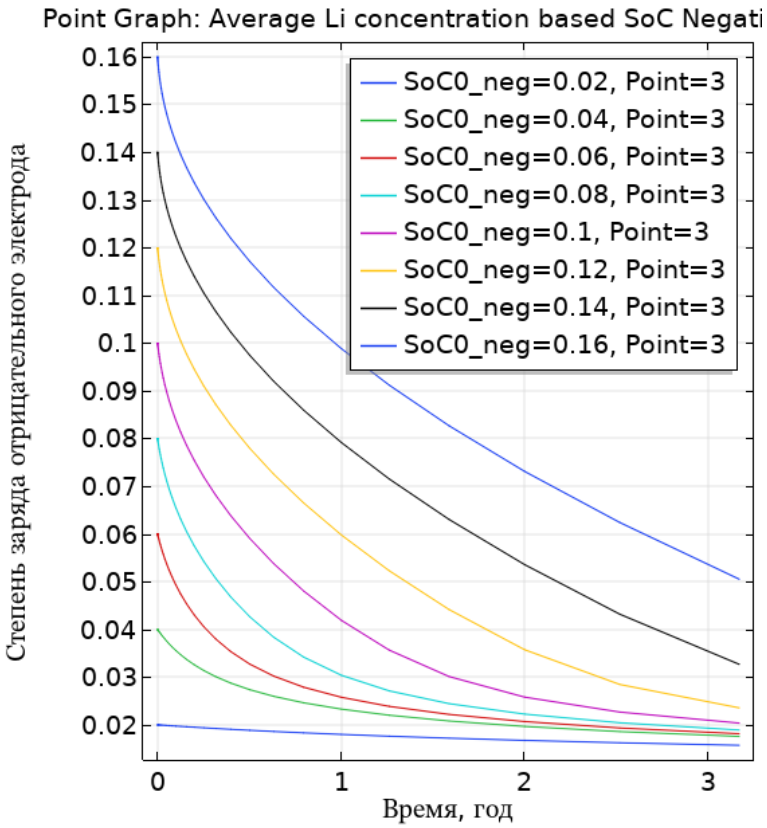


***Figure 26. Dependence of the degree of charge of the negative electrode on time***

When SoC_neg <0.04, the rate of lithium reduction decreases. This is caused by the fact that the closer SoC_neg comes to 0, the more U_ocp_neg increases (Figure 4) and the reaction speed slows down.

### 5.3.2. DC charging and relaxation

Let's consider charging with a 1C current (direct current that fully charges the battery in 1 hour) and subsequent relaxation. Instead of sequentially simulating a large number of charges, we will simulate a single charge and determine how quickly the SEI layer grows in 1 cycle (104 seconds to be specific) depending on the initial film thickness. In this formulation of the problem, it is necessary that the total amount of lithium (in the electrodes, electrolyte and film) remains constant. Accordingly, when the initial concentration of the film changes, it is necessary to recalculate the concentration of lithium contained in graphite so that the integral value of the amount of lithium does not change. This is what we will check first before analyzing the results. According to the data from Table 6, the total amount of

lithium in the electrodes, electrolyte and SEI is the same when varying the parameter of the initial film thickness.

***Table 6. Total amount of lithium when varying the initial film thickness.***

| Initial concentration of SEI layer, mol/m^2 | Total amount of lithium, mol/m^2 |
|---|---|
| 0 | 1.4046 |
| 50 | 1.4046 |
| 100 | 1.4046 |
| 150 | 1.4046 |
| 200 | 1.4046 |
| 250 | 1.4046 |
| 300 | 1.4046 |
| 350 | 1.4046 |
| 400 | 1.4046 |
| 450 | 1.4046 |
| 500 | 1.4046 |

Figure 27 shows battery charging graphs for various initial SEI layer thicknesses.

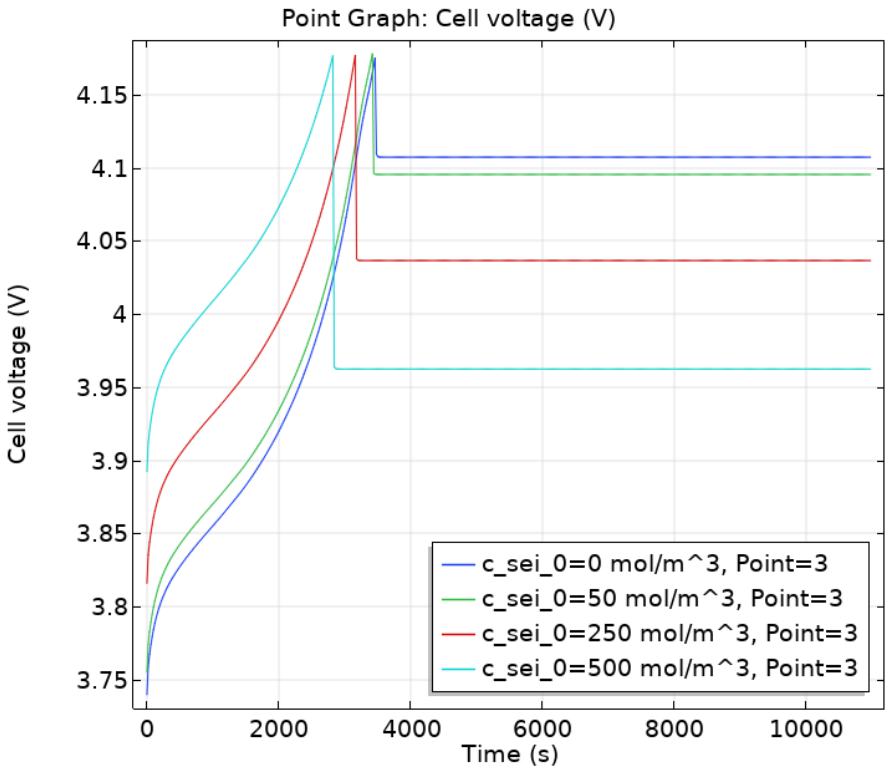


***Figure 27. Charging cycles for different initial film concentrations***

In addition to the resistance of the battery as a whole, the film also has a resistance at which an additional potential drop occurs, which disappears when the current is turned off. This potential jump on the film prevents the battery from being fully charged in this formulation of the problem (stopping charging when the threshold voltage is reached). At the same time, with a layer thickness of 500 mol/m3 (440 nm), the battery reaches a lower voltage (3.95 V instead of 4.12 V) and requires less current supply time by 500 seconds.

### 5.3.3. Constant current and constant voltage charging

Having considered DC charging, we came to the conclusion that this implementation is not enough to complete the charging cycle (due to the presence of ohmic resistance). To fully charge the battery, constant current charging was used in combination with constant voltage charging. It is produced by a current of 1C until the stopping voltage, and then in constant voltage mode the battery is recharged. Details about the implementation of this method can be found in part 4.7.

To begin with, let us compare the film growth rates for 1 charging cycle for all presented types: charging with constant current, voltage and relaxation - depending on the initial layer thickness. If it turns out that the SEI layer grows at the same rate regardless of the type of charging, then it will be possible to significantly simplify the implementation of the film model, take advantage of time acceleration and significantly reduce modeling time.

Let's set the same calculation time for all processes (104 seconds) so that we can correctly compare all grown layers per cycle. A graph of the increment in film layer thickness after 1 charge as a function of the initial film layer for the new type of charge is shown in Figure 28.

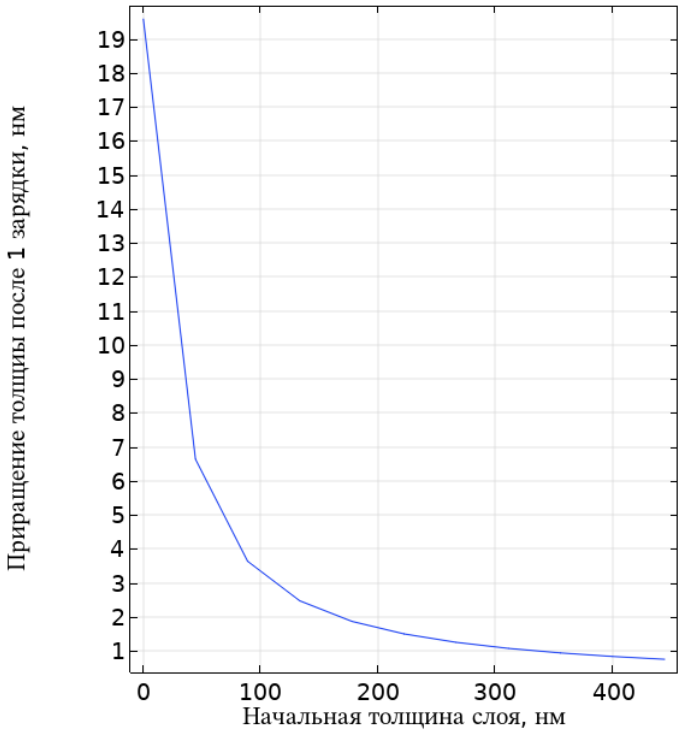


***Figure 28. Varying the amount of the grown layer in 1 cycle from the existing one.***

Let us now compare the available data for the increment of layers with similar results obtained for other processes over a similar period of time. The data is presented in Figures 29,30.


***Figure 29.Deviations in layer growth for different charging cycles in absolute values (cycle time 10,000 seconds). Charging with constant current, charging with constant current + then constant voltage and no current are compared***


***Figure 30. Deviations in layer growth for different charging cycles in relative values***

Based on this graph, it is noticeable that there is a noticeable difference in the first charge cycles, when the thickness of the SEI layer is less than 200 nm, but when this is reached, the relative differences in the growth rate are insignificant. When the film thickness reaches 200 nm, film growth ceases to depend on how the battery is used. This means that when this thickness is reached, you can use the time acceleration specified in part 4.5.2.

### 5.3.4. DC charge/discharge

Let's consider the last operating mode - charge/discharge with direct current. The film layer growth graph is shown in Figure 31.

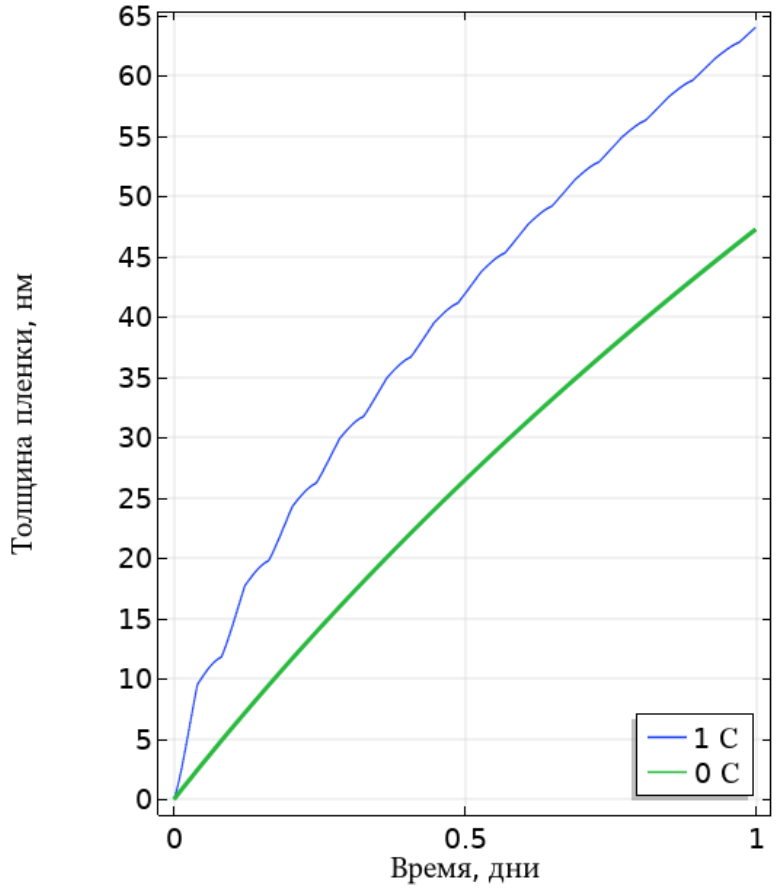


***Figure 31. Recharging schedule with currents of 1C and 0C***

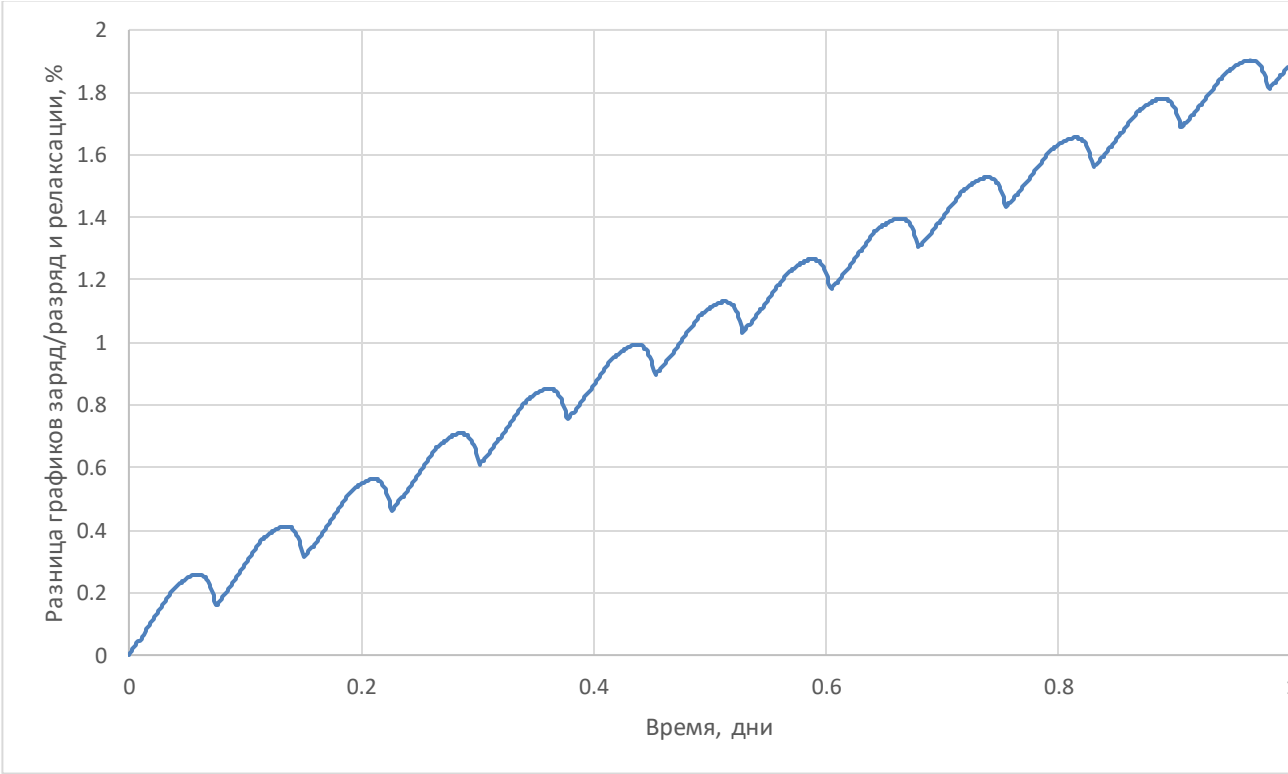


***Figure 32 .Relative value of film growth during a charge/discharge cycle compared to growth in the absence of current at an initial film layer of 200 nm***

Figure 31 clearly shows that when charging, the growth rate of the film layer in the first cycles is much faster than the growth of the film when the battery is discharged (blue graph). Moreover, the highest speed is shown when charging an almost discharged capacitor. However, once the thickness reaches 60 nm (10 cycles), the difference between charging and discharging is no longer noticeable. It is worth noting that a similar graph (Figure 7) was also shown in the article [14]. Presented on the same axes, the film growth plot in the absence of current (green) is noticeably different from the charge/discharge modes. In the first day the difference was more than 130%. However, then the growth rates of the graphs become similar. Let's evaluate the difference between the layers grown with the already existing initial layer of SEI 200 nm (Figure 32). Over the course of a day (13 charge/discharge cycles), the difference between the increases is less than 2%. These data, when combined with Figure 30, show little difference in film growth across all charging cycles for a film thickness of 200 nm.

Main conclusion: with this set of parameters, when the film thickness reaches 200 nm, the difference between all battery operating modes becomes insignificant, and further growth can be described by a model with no current (it is calculated much faster). When SoC_neg reaches a value of 0.04 (4-6%), a significant increase in U_ocp_neg occurs, preventing lithium from leaving the negative electrode. All this causes the growth rate of the SEI film to decrease, as shown in the graph. To reduce the film growth rate, the SoC_neg0 value should be 0.02 higher than 0.04 to achieve a maximum film thickness in the region of 500 nm. However, this reduction in the amount of active lithium may negatively affect the battery capacity.

## 5.4. Battery capacity drop

During the study in the section “Various charging cycles”, the dependence of the film growth rate on the amount of lithium filling of the negative electrode was determined (Figure 25). When decreasing the SoC_neg value from 0.12 to 0.04 in the relaxation mode, the film thickness after 3 years changes by an order of magnitude (from 2.6 μm to 400 nm). It is quite clear that the battery capacity is

proportional to the amount of lithium it contains. The film, in turn, Due to the occurrence of side reactions, it reduces the amount of lithium in the electrodes, which can participate in the recharging process. This section will be devoted to identifying the dependence of battery capacity on film thickness and the amount of lithium in the electrodes.

The experiment was modeled as follows. To begin with, the battery with varied parameters was charged with direct current for one hour until fully charged (this current is abbreviated as 1C), and was brought to a voltage of 4.18 V until fully charged. Then, from a time of 104 seconds, the battery was discharged with a direct current of 1C to a voltage of 3.5 V. The graph is presented in Figure 33.

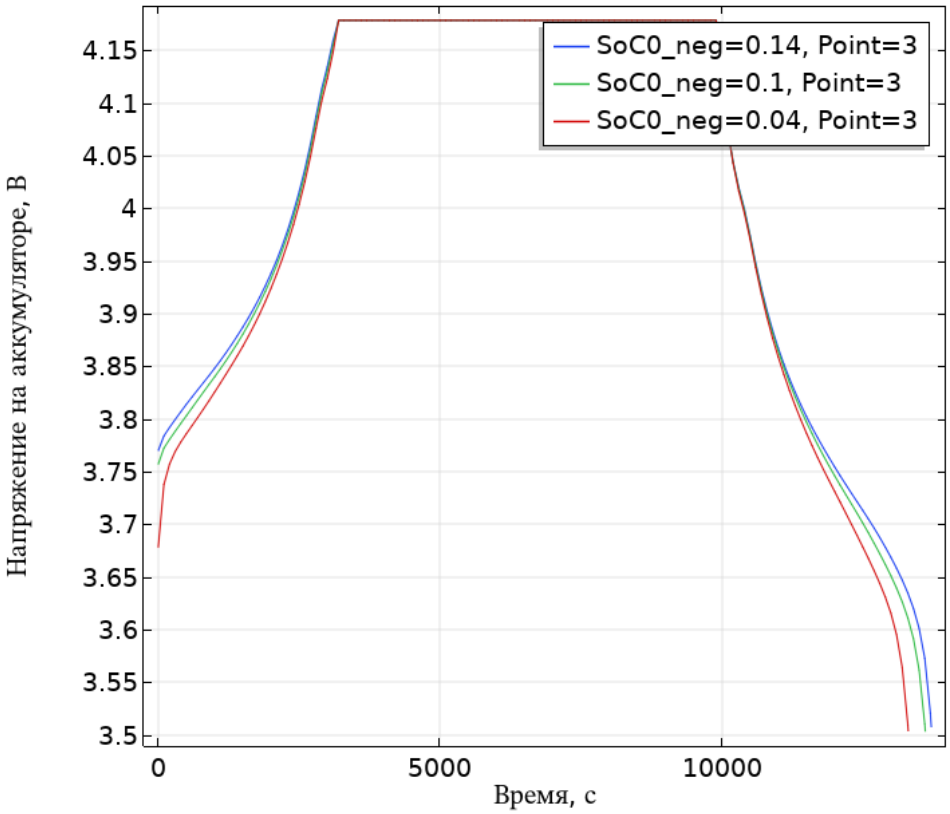


***Figure 33a. Voltage graph of the entire experiment***

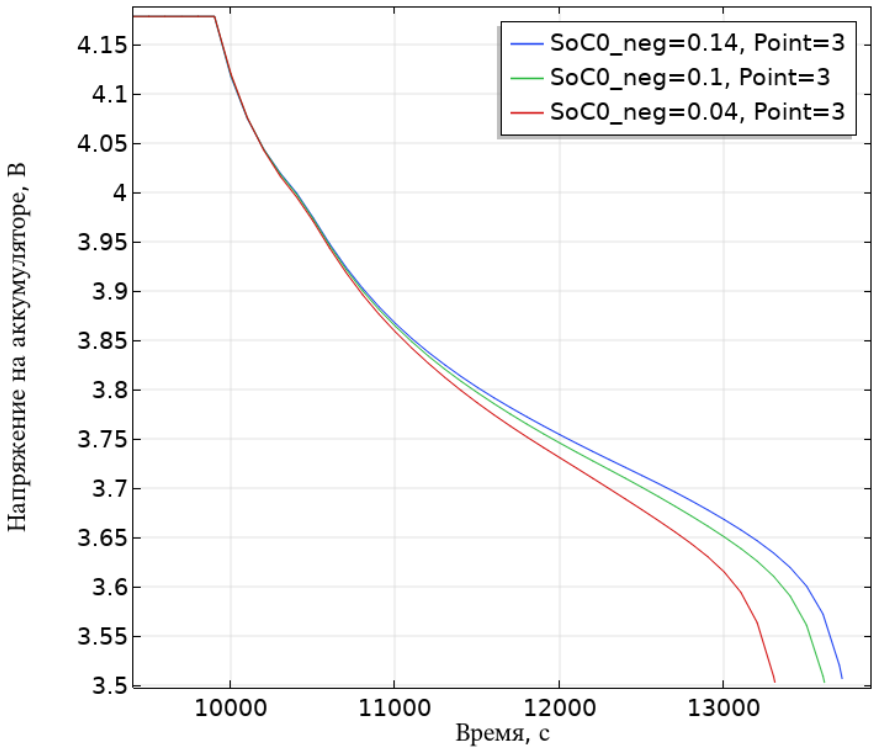


***Figure 33b. Graph of the part of the experiment corresponding to battery discharge***

The capacity of the battery was determined through the time that the battery a given current could support

$$Q(i_{app}, U_{start}, U_{stop}) = i_{app} \cdot time_{dch}$$

Where $i_{app}, time_{dch}$ are the current and discharge time, and $U_{start}, U_{stop}$ are the initial and final voltages.

We will also additionally check the dependency of the battery capacity on amount of lithium. In the future, it turns out that capacity will begin to be lost only when a certain amount of lithium is reached (SoC_neg = 0.04 in Figure 4b), starting from which the value of U_ocp(SoC_neg) increases sharply. In other cases, the capacity will remain.

### 5.4.1. Varying layer thickness

Let us plot the dependence of the relative capacitance on the thickness of the film layer.

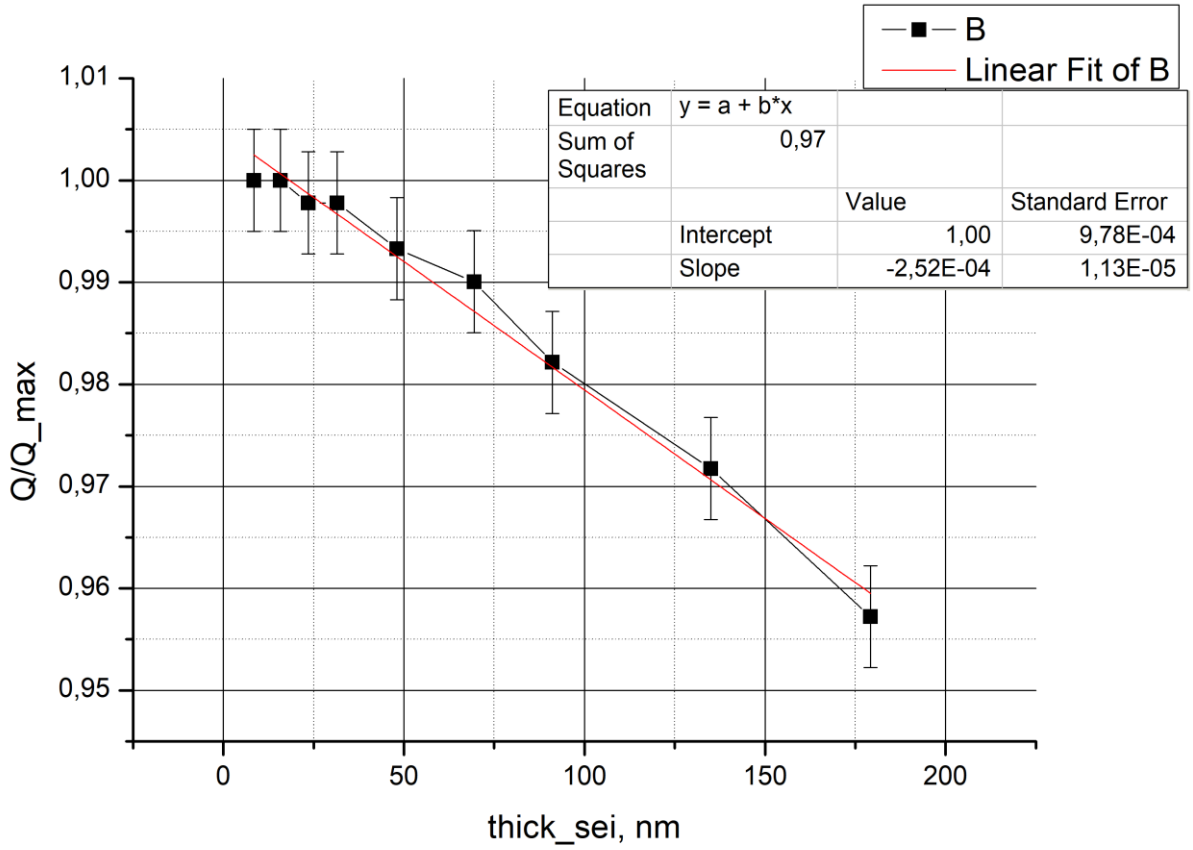


***Figure 34. Graph of relative capacitance versus film thickness at fixed SoC0_neg = 0.05***

The graph in Figure 34 is a linear function. This happens due to the fact that additional voltage drops on the film, which limits the use of this battery in the proposed discharge setting to a certain voltage. The error in capacity calculation is associated with the last point in the solution. The program does not calculate the last step when the required voltage value is reached. The relative amount of lithium depending on the film thickness is given in Table 7.

***Table 7. Relative amount of lithium depending on film thickness.***

| c_sei_avg, mol/m3 | Li/Li_max |
|---|---|
| 9.6 | 1.000 |
| 17.8 | 1.000 |
| 26.4 | 0.999 |
| 35.4 | 0.999 |
| 54.0 | 0.999 |
| 78.0 | 0.998 |
| 102.4 | 0.997 |
| 151.7 | 0.995 |
| 201.3 | 0.994 |

The amount of lithium decreased by about 0.5% when the capacity changed, determined by current, by 5% (Figure 34). Therefore, capacity loss cannot be measured due to a decrease in its “bulk”.

### 5.4.2. Varying the degree of lithium filling.

We will vary the initial degrees of lithium filling of the positive and negative electrodes and determine how the battery capacity depends on the amount of available lithium.

To begin with, consider a graph of the dependence of the relative capacitance on the final value of SoC_neg, which determines the degree of lithium filling of the negative electrode.

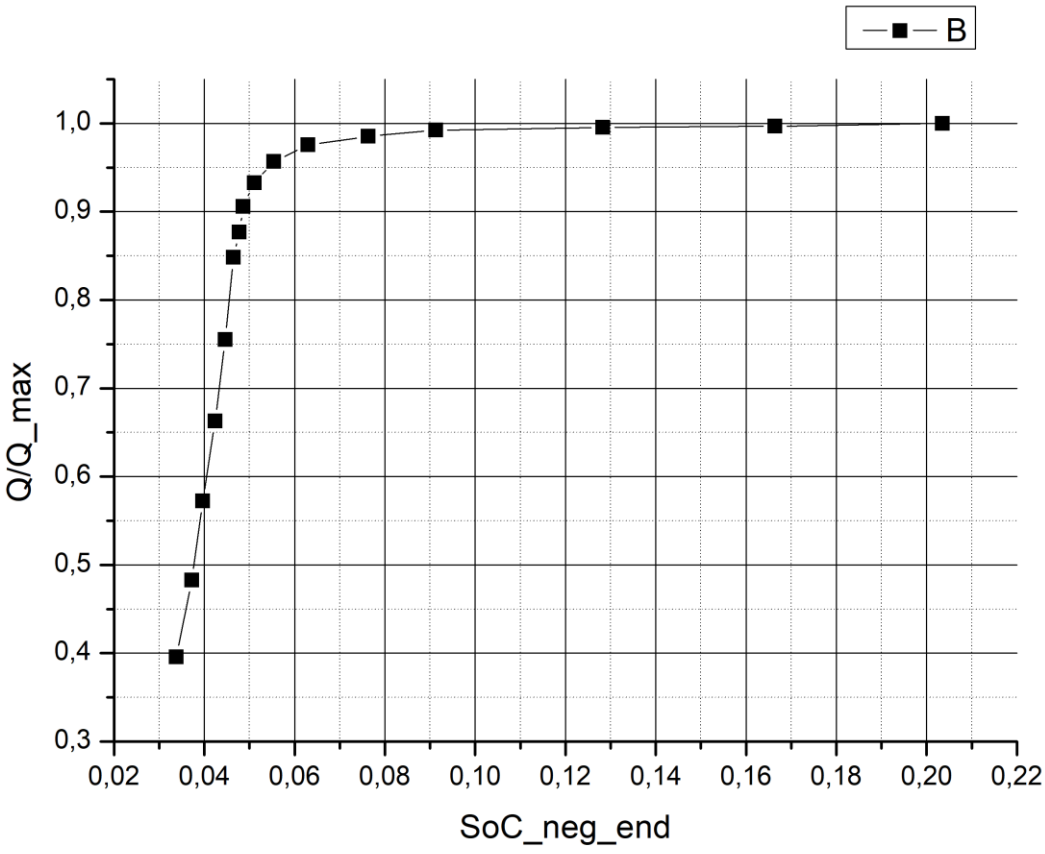


***Figure 35. Dependence of relative capacitance on the final value of SoC_neg***

Depending on the amount of lithium at the last moment of time (Figure 35), the battery capacity is near its maximum value (with SoC_neg > 0.08) or drops sharply

when the value SoC_neg ~ 0.04 is reached. It turns out that one of two situations is possible:

- The battery does not lose capacity, having a certain supply of lithium in the negative electrode area
- The battery is discharged to SoC_neg = 0.04

This graph encourages the analysis of the dependence of capacity on the amount of lithium in the electrodes.

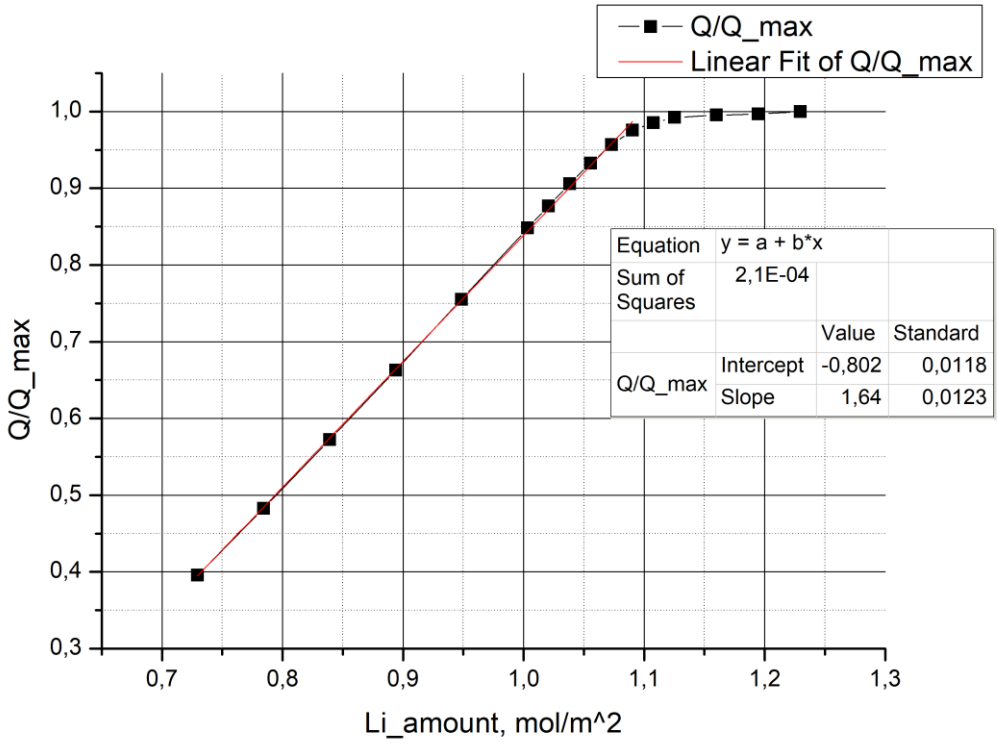


***Figure 36. Graph of relative capacitance versus the total amount of lithium in the electrodes***

Based on the data presented in Figure 36, we can conclude that when the amount of lithium is >1.1 mol/m^2 for a given battery configuration, its capacity has a constant value. As the amount of lithium decreases, it begins to decrease linearly (provided that there is no film layer). A value of 1.1 mol/m^2 of lithium corresponds to a fully charged positive electrode and a negative electrode charged by 4-6% (the moment of a sharp increase in the open circuit voltage in Figure 4b.

# 6. Conclusions

The presented SEI models based on solvent diffusion through the film describe well the presented experimental data [9, 14]. However, consideration of these data was limited to a small set of experimental values (for example, the dependence of the capacitance drop on time).

The new result of the work is the created module taking into account battery degradation during its use. By changing the coefficients, it is possible to obtain SEI models similar to those described in the literature. This model can also be improved, for example, by taking into account cracks in the layer, as in [15]. This implementation of film growth over time, when combined with a heat calculation module, can give an idea of the failure rate of real batteries.

During the analysis of the model, it was found that the key factor for film growth and loss of battery capacity is not only the diffusion coefficient and reaction rate, but also the amount of stored lithium in the solid phase. Starting from a certain amount of lithium, its capacity stops growing (Figure 34). For this configuration, this value is about 1.1 mol/m2. Which corresponds to a fully charged positive electrode and 4-6% negative. Reducing the amount of lithium due to the formation of the SEI layer leads to a loss of capacity.

With different degrees of charge on the negative electrode, the growth rate of the SEI layer also changes greatly (Figure 25). The layer thickness at a charge level of 4% and 12% after 3 years (characteristic operating time) differs by an order of magnitude (500 nm versus 2300 nm).

When the thickness of the SEI layer reaches about 200 nm, the difference in the growth of the SEI layer during different charging or discharging cycles becomes insignificant (provided that the processes take the same amount of time) (Figures 30 and 32). Accordingly, after reaching a given layer thickness, you can simplify the calculation of the problem by adding the time acceleration implemented in part 4.5.2. However, for small layer sizes it is not recommended to use such a simplification. If the SEI thickness at large times is of interest, then we can immediately calculate with time acceleration. The film growth rate decreases with increasing film

thickness. Even if the solutions differ at the initial moments, over time the difference will disappear.

If it is possible to store a large amount of additional lithium in the battery, a twofold situation arises: on the one hand, the more excess lithium can be stored in the battery, the later it will begin to lose its capacity. However, this solution will lead to rapid growth of the film layer and the release of more heat on it as a result of ohmic heating.

It turns out that in order to create a battery that will retain capacity for a long time, operating at optimal temperatures without the risk of overheating, you need to add as much lithium as possible. On the other hand, to create a battery for operation in adverse conditions, where overheating is critical, it is worth avoiding a large amount of lithium, due to which an excess film is formed on the electrode.

# 7. Applications

## Appendix 1. Derivation of the equation for solvent concentration near the electrode

Let us consider the transport equation of solution molecules through the film.

$$\frac{\partial c_{sol}(\mathrm{x,t})}{\partial t} = -\frac{\partial W(x,\mathrm{t})}{\partial x}$$

Where is the flux density of electrolyte particles (consists of 2 parts: diffusion and convective part, because the wall itself moves away), is the film withdrawal rate, is the layer thickness sei

$$\mathrm{W(x,t)} = -D \cdot \frac{\partial c_{sol}(\mathrm{x,t})}{\partial x} + v \cdot c_{sol}(\mathrm{x,t})$$

$$v(x,t) = \frac{d\Delta l_{sei}(x,t)}{dt}\Delta l_{sei}(x,t)$$

$$\frac{\partial c_{sol}}{\partial t} = D_{sei} \cdot \frac{\partial^2 c_{sol}}{\partial x^2} - v \cdot \frac{\partial c_{sol}}{\partial x}$$

Let the electrolyte concentration clearly not depend on time. Then

$$D_{sei} \cdot \frac{d^2 c_{sol}}{dx^2} - v \cdot \frac{dc_{sol}}{dx} = 0$$

System solution:

$$c_{sol} = C_1 + C_2 \cdot \exp\left(\frac{1}{D_{sei}} \cdot v \cdot x\right) \sim C_1 + C_2 \cdot (1 + \frac{1}{D_{sei}} \cdot v \cdot x)$$

Let us limit ourselves to 2 terms of the expansion. Boundary conditions:

$$\mathrm{C}_1 + \mathrm{C}_2 = c_{solvent}$$

$$C_1 + C_2 \cdot \left(1 + \frac{1}{D_{sei}} \cdot v \cdot \Delta l_{sei}\right) = c_0$$

Or

$$\mathrm{c}(x) = c_{elec} + C_2 \cdot \frac{1}{D_{sei}} \cdot v \cdot x$$

Let's find the factor C2:

1st Fick's law:

$$\mathrm{j} = -D\frac{\partial c}{\partial x}$$

Then

$$j_{sei} \cdot \frac{M_{sei}}{M_{solvent}} = j_{elec} = -D_{sei} \cdot C_2 \cdot \frac{1}{D_{sei}} \cdot v \cdot \frac{dx}{dx} = C_2 \cdot v$$

$$\frac{\rho_{sei}}{M_{solvent}} = C_2$$

Total

$$\mathrm{c}_{solvent} = c_0 \cdot \left(1 - \frac{\rho_{sei} \cdot \Delta l \cdot v}{M_{solvent} \cdot c_0 \cdot D}\right) = c_0 \cdot \left(1 - Z \cdot \frac{dc_{sei}}{dt} \cdot c_{sei}\right)$$

Where

$$Z = \left(\frac{M_{sei}}{a_{as}}\right)^2 \cdot \frac{1}{\rho_{sei} \cdot M_{solvent} \cdot c_0 \cdot D_{sei}}$$

# 8. References

[1]Doyle, M., Fuller, T. F., & Newman, J. (1993). Modeling of Galvanostatic Charge and Discharge. Journal of the Electrochemical Society, 140(6), 1526–1533., 1993

[2]Doyle, M., Newman, J., Gozdz, A. S., Schmutz, C. N., & Tarascon, J. (1996). Comparison of Modeling Predictions with Experimental Data from Plastic Lithium Ion Cells. Journal of The Electrochemical Society, 143(6), 1890–1903. https://doi.org/10.1149/1.1836921, 1996

[3]Wang, Y., Nakamura, S., Ue, M., & Balbuena, P. B. (2001). Theoretical studies to understand surface chemistry on carbon anodes for lithium-ion batteries: Reduction mechanisms of ethylene carbonate. Journal of the American Chemical Society, 123(47), 11708–11718. https://doi.org/10.1021/ja0164529, 2001

[4]Novák, P., Joho, F., Imhof, R., Panitz, J. C., & Haas, O. (1999). In situ investigation of the interaction between graphite and electrolyte solutions. Journal of Power Sources, 81–82, 212–216. https://doi.org/10.1016/S0378-7753(99)00119-6, 1999

[5]Kumaresan, K., Sikha, G., & White, R. E. (2008). Thermal Model for a Li-Ion Cell. Journal of The Electrochemical Society, 155(2), A164. https://doi.org/10.1149/1.2817888, 2008

[6]Li, B., Chao, Y., Li, M., Xiao, Y., Li, R., Yang, K., Cui, X., Xu, G., Li, L., Yang, C., Yu, Y., Wilkinson, D. P., & Zhang, J. (2023). A Review of Solid Electrolyte Interphase (SEI) and Dendrite Formation in Lithium Batteries. In Electrochemical Energy Reviews (Vol. 6, Issue 1). Springer Nature Singapore. https://doi.org/10.1007/s41918-022-00147-5, 2023

[7]Heiskanen, S. K., Kim, J., & Lucht, B. L. (2019). Generation and Evolution of the Solid Electrolyte Interphase of Lithium-Ion Batteries. Joule, 3(10), 2322–2333. https://doi.org/10.1016/j.joule.2019.08.018, 2019

[8]Plett, G. (2015). Battery Management Systems, Volume I Battery Modeling., 2015

[9]Pinson, M. B., & Bazant, M. Z. (2013). Theory of SEI Formation in Rechargeable Batteries: Capacity Fade, Accelerated Aging and Lifetime Prediction. Journal of The Electrochemical Society, 160(2), A243–A250. https://doi.org/10.1149/2.044302jes, 2013

[10] Li, D., Danilov, D., Zhang, Z., Chen, H., Yang, Y., & Notten, P. H. L. (2015). Modeling the SEI-Formation on Graphite Electrodes in LiFePO 4 Batteries. Journal of The Electrochemical Society, 162(6), A858–A869. https://doi.org/10.1149/2.0161506jes, 2015

[11] Köbbing, L., Latz, A., & Horstmann, B. (2023). Growth of the solid-electrolyte interphase: Electron diffusion versus solvent diffusion. Journal of Power Sources, 561, 232651. https://doi.org/10.1016/j.jpowsour.2023.232651, 2023

[12] Fedorova, A. A., Anishchenko, D. V., Beletskii, E. V., Kalnin, A. Y., & Levin, O. V. (2021). Modeling of the overcharge behavior of lithium-ion battery cells protected by a voltage-switchable resistive polymer layer. Journal of Power Sources, 510. https://doi.org/10.1016/j.jpowsour.2021.230392, 2021

[13] Cai, L., & White, R. E. (2011). Mathematical modeling of a lithium ion battery with thermal effects in COMSOL Inc. Multiphysics (MP) software. Journal of Power Sources, 196(14), 5985–5989. https://doi.org/10.1016/j.jpowsour.2011.03.017, 2011

[14] Liu, L., Park, J., Lin, X., Sastry, A. M., & Lu, W. (2014). A thermal-electrochemical model that gives spatial-dependent growth of solid electrolyte interphase in a Li-ion battery. Journal of Power Sources, 268, 482–490. https://doi.org/10.1016/j.jpowsour.2014.06.050, 2014

[15] Ekström, H., & Lindbergh, G. (2015). A Model for Predicting Capacity Fade due to SEI Formation in a Commercial Graphite/LiFePO 4 Cell. Journal of The Electrochemical Society, 162(6), A1003–A1007. https://doi.org/10.1149/2.0641506jes, 2015

[16] Jiang, G., Zhuang, L., Hu, Q., Liu, Z., & Huang, J. (2020). An investigation of heat transfer and capacity fade in a prismatic Li-ion battery based on an electrochemical-thermal coupling model. Applied Thermal Engineering, 171(February), 115080. https://doi.org/10.1016/j.applthermaleng.2020.115080, 2020

[17] Borodin, O., Smith, G. D., & Fan, P. (2006). Molecular dynamics simulations of lithium alkyl carbonates. Journal of Physical Chemistry B, 110(45), 22773–22779. https://doi.org/10.1021/jp0639142, 2006

[18] Lam, L. L. (2014). Determining optimal discharge strategy for rechargeable lithium-ion batteries using multiphysics simulation.